STEM CELLS AND DEVELOPMENT
Volume 21, Number 16, 2012

DOI: 10.1089/scd.2011.0725

Nucleostemin in Injury-Induced Liver Regeneration

Haruhiko Shugo,[1,2,*] Takako Ooshio,[1,*] Masako Naito,[1] Kazuhito Naka,[1] Takayuki Hoshii,[1] Yuko Tadokoro,[1] Teruyuki Muraguchi,[1] Akira Tamase,[1] Noriyuki Uema,[1] Taro Yamashita,[2] Yasunari Nakamoto,[2] Toshio Suda,[3] Shuichi Kaneko,[2] and Atsushi Hirao[1]

The high regenerative capacity of liver contributes to the maintenance of its size and function when injury occurs. Partial hepatectomy induces division of mature hepatocytes to maintain liver function, whereas severe injury stimulates expansion of undifferentiated hepatic precursor cells, which supply mature cells. Although several factors reportedly function in liver regeneration, the precise mechanisms underlying regeneration remain unclear. In this study, we analyzed expression of nucleostemin (NS) during development and in injured liver by using transgenic green fluorescent protein reporter (NS-GFP Tg) mice. In neonatal liver, the hepatic precursor cells that give rise to mature hepatocytes were enriched in a cell population expressing high levels of NS. In adult liver, NS was abundantly expressed in mature hepatocytes and rapidly upregulated by partial hepatectomy. Severe liver injury promoted by a diet containing 3,5-diethoxycarbonyl-1,4-dihydrocollidine induced the emergence of NS-expressing ductal epithelial cells as hepatic precursor cells. NS knockdown inhibited both hepatic colony formation in vitro and proliferation of hepatocytes in vivo. These data strongly suggest that NS plays a critical role in regeneration of both hepatic precursor cells and hepatocytes in response to liver injury.

Introduction

THE LIVER IS AN ORGAN WITH high regenerative capacity, enabling it to maintain a constant size and function following injury [1,2]. In resting liver, hepatocytes are quiescent and rarely undergo cell division. Therefore, hepatocyte replacement occurs slowly in static conditions. However, when the liver is injured, cells replicate to restore loss of tissue mass and function. Proliferation of hepatocytes and bile duct epithelial cells contributes to liver maintenance. After partial hepatectomy, the remaining lobes regenerate the entire liver mass within 5–7 days, a process accomplished primarily by division of mature cells rather than of stem/precursor cells. In mice, division of hepatocytes starts after partial hepatectomy and is maximal 24–48 h later. Several molecules, including hepatocyte growth factor (HGF), interleukin-6, tumor necrosis factor α, transforming growth factor, and epidermal growth factor (EGF), reportedly govern this process [1,2]. Termination of regeneration is also important for the maintenance of homeostasis. In severe injury associated with defects in hepatocyte proliferation, it is believed that bipotential precursors of hepatocytes and cholangiocytes contribute to liver regeneration [3,4]. Currently, it is thought that potential hepatic precursor cells emerge from smaller branches of the biliary tree. In rats, a population of small cells exhibiting large nuclei, called oval cells, emerges around portal veins following liver injury [5]. In mice, a diet supplemented with 3,5-diethoxycarbonyl-1,4-dihydrocollidine (DDC) induces ductal proliferation and morphological changes similar to those seen in the rat oval cell response [6]. Precursor cells appear to regenerate hepatocytes and cholangiocytes through proliferation, migration, and differentiation processes. Thus, proper control of both mature cells and hepatic stem/precursor cells is critical for liver regeneration.

Nucleostemin (NS) is a GTPase that binds to p53 and was originally reported to be highly expressed in stem cells from several tissues, including embryonic stem (ES) cells, immature hematopoietic cells, and neural stem/progenitor cells [7]. NS loss results in reduced cell proliferation and increased apoptosis in both ES cells and ES cell-derived neural stem/progenitor cells [8]. Structural comparisons have been used to isolate NS homologues in *Caenorhabditis elegans* [9], newt [10], *Xenopus* [11], mouse [7], and human [12]. In the regenerating newt lens, NS protein rapidly accumulates in nucleoli of dedifferentiating pigmented epithelial cells and multinucleate muscle fibers [10], suggesting that its expression correlates with undifferentiated status in newt cells. In contrast, the NS homologue in *Caenorhabditis elegans* (*nst-1*) is expressed in both proliferating and differentiated cells. *Nst-1* mutants exhibit defects in larval growth and cell cycle

[1]Division of Molecular Genetics, Cancer Research Institute, Kanazawa University, Kanazawa, Japan.
[2]Disease Control and Homeostasis, Kanazawa University Graduate School of Medical Science, Kanazawa, Japan.
[3]Department of Cell Differentiation, The Sakaguchi Laboratory of Developmental Biology, Keio University School of Medicine, Tokyo, Japan.
*These authors contributed equally to this work.

progression in germline stem cells [9]. Because *nst-1*-mutant germ cells can still differentiate into mature sperm, nst-1 may play a critical role in germline stem cell proliferation but not in differentiation. In addition, NS is reportedly expressed at similar levels in non-proliferating muscle stem cells (satellite cells), rapidly proliferating precursor cells (myoblasts), and post-mitotic terminally differentiated cells (myotubes and myofibers) [13]. NS downregulation inhibits differentiation of myoblasts to myotubes, suggesting a role in post-mitotic terminal differentiation in this type. Thus, NS has pleiotropic effects on cellular function, and it is unclear how NS is involved in cell differentiation.

In a previous study, we generated a reporter system where the NS promoter drives green fluorescent protein (GFP) expression (termed NS-GFP) in vivo [14]. We successfully used this reporter system to identify a specific fraction of neonatal germ cells as spermatogonial stem cells with long-term repopulating capacity. We also combined the NS reporter system with a mouse brain tumor model and demonstrated the existence of an undifferentiated tumor-initiating cell (TIC) population in a highly aggressive brain tumor by analyzing GFP fluorescence intensity [15]. Consistent with our data, a recent report employing a bacterial artificial chromosome transgenic mouse line expressing GFP from the NS promoter showed that NS-enriched mammary tumor cells are highly tumorigenic in vitro and in vivo [16]. Further, another recent report showed that NS overexpression enhanced tumorigenicity of TICs, increased expression of genes that maintain undifferentiated status, and enhanced radioresistance [17]. These data suggest that NS functions to maintain stem cell properties in malignant cells.

In this study, we examined the expression and function of NS in liver. Interestingly, we found that NS contributes to the proliferation of hepatocytes after partial hepatectomy and to the regenerative capacity of hepatic precursor cells. Our data strongly suggest that NS is essential for injury-induced liver regeneration.

Materials and Methods

Animals

Mice used in this study were on a C57BL/6 background. NS-GFP Tg mice were generated as described previously [14]. Livers were collected at fetal (embryonic day 14.5: E14.5), neonatal (postnatal day 5: P5), and adult (8 weeks old) stages. For experiments involving severe liver injury, adult mice were fed a diet containing 0.1% DDC (Sigma-Aldrich, St. Louis, MO) for 2 weeks [6]. For partial hepatectomy, mice were anesthetized and 70% of the liver was resected. All procedures were performed in accordance with the animal care guidelines of Kanazawa University.

Isolation of liver cells

For digestion of fetal or neonatal liver cells, livers were minced and dissociated with enzyme-based dissociation buffer (Invitrogen Life Technologies, Carlsbad, CA) as described previously [18]. For isolation of adult liver cells, a 2-step perfusion method was utilized [19]. Briefly, perfusion collagenase solution (0.5 g/L; Sigma-Aldrich) was administered to a sacrificed mouse via the portal vein. Nonparenchymal cells were separated from parenchymal cells by centrifugation (50 *g*, 1 min), and dead cells were removed by centrifugation through 25% Percoll solution (GE Healthcare, Tokyo, Japan).

Flow cytometry

Single-cell suspensions from fetal, neonatal, or adult liver were incubated with an anti-CD16/CD32 antibody on ice for 10 min, followed by incubation with phycoerythrin (PE)-conjugated anti-TER119 and anti-CD45 antibodies (BD Pharmingen, San Diego, CA) on ice for 30 min. Cells were washed thrice in staining solution [2% fetal calf serum (FCS)/phosphate-buffered saline (PBS)] and incubated with anti-PE microbeads (Miltenyi Biotech, Bergisch Gladbach, Germany). After 3 washes, $CD45^{-}TER119^{-}$cells were collected (MACS; Miltenyi Biotech). Fetal liver cells were incubated with a biotin-conjugated anti-Dlk antibody (MBL, Nagoya, Japan), followed by incubation with allophycocyanin-conjugated streptavidin antibody (BD Pharmingen). Dead cells were stained with propidium iodide. Fluorescence-labeled cells were analyzed and sorted with JSAN (Bay Bioscience Co, Kobe, Japan).

Hepatic colony forming assay

Cells fractionated by flow cytometry were inoculated at 2,500 cells/well into six-well dishes coated with type I collagen (0.3 mg/mL; Nitta Gelatin, Osaka, Japan). The culture medium included Dulbecco's modified Eagle medium (DMEM)/F-12 supplemented with 10% fetal bovine serum, 5 mmol/L HEPES (Wako, Osaka, Japan), 200 μmol/L L-glutamine (Invitrogen Life Technologies), 50 μmol/L 2-mercaptoethanol (Sigma-Aldrich), 10 mmol/L nicotinamide (Sigma-Aldrich), 10^{-7} mol/L dexamethasone (Sigma-Aldrich), 1 mg/L insulin (Wako), 1× penicillin/streptomycin (Invitrogen Life Technologies), 50 ng/mL HGF (Peprotech, Rocky Hill, NJ), and 20 ng/mL EGF (Sigma-Aldrich).

Immunohistochemical analyses

Adult liver tissues were fixed with 4% paraformaldehyde at 4°C overnight and embedded in paraffin. Frozen sections were sliced and then fixed with 4% paraformaldehyde. The following primary antibodies were used: goat anti-NS (1:200; R&D Systems, Inc., Minneapolis, MN), rabbit anti-GFP (1:500; Invitrogen Life Technologies), and mouse anti-Ki-67 (1:200; BD Pharmingen). Sections were incubated with primary antibodies for 16 h at 4°C, followed by incubation with the appropriate Alexa Fluor dye conjugated to anti-goat IgG, anti-rabbit IgG, or anti-mouse IgG secondary antibodies (all 1:200; Molecular Probes, Inc., Eugene, OR). Staining was visualized using confocal microscopy (FV1000; Olympus, Tokyo, Japan). For some experiments, primary antibodies were detected using peroxidase-conjugated secondary antibodies (GE Healthcare, Amersham, Buckinghamshire, UK) in combination with a 3, 3'-diaminobenzidine (DAB) Peroxidase Substrate Kit (Vector Laboratories, Burlingame, CA). Sections were counterstained with Mayer's hematoxylin and analyzed using a microscope (Ax80; Olympus).

Immunocytochemical analyses

Hepatic colonies or cell lines were fixed with 4% paraformaldehyde for 10 min, followed by incubation with goat anti-albumin (1:100; Bethyl Laboratories, Montgomery, TX),

rabbit anti-cytokeratin 19 (1:1,000, a gift from Dr. Atsushi Miyajima), chicken anti-GFP (1:500; AVES, Tigard, OR), and/or mouse anti-Ki-67 (1:200; BD Pharmingen) at 4°C overnight and then stained with Alexa 546–conjugated and/or Alexa 488–conjugated secondary antibodies.

Western blotting analyses

Liver samples were lysed with sodium dodecyl sulfate (SDS)–polyacrylamide gel electrophoresis (PAGE) sample buffer, sonicated, boiled, and used as total liver cell lysates. Protein concentrations were measured by the bicinchoninic acid (BCA) protein assay (Pierce, Rockford, IL), and equal amounts of protein were separated by SDS-PAGE and transferred onto polyvinylidene difluoride (PVDF) membranes. Membranes were blocked with 5% skim milk in PBS containing Tween 20 for 1 h at room temperature. Membranes were then incubated with a goat anti-NS antibody (1:1,000; Neuromics, Edina, MN) for 16 h at 4°C and a mouse anti-β-actin antibody (1:1,000; Sigma-Aldrich) for 1 h at room temperature. Immune complexes were detected using peroxidase-conjugated secondary antibodies (1:1,000; GE Healthcare and DAKO, Glostrup, Denmark) for 30 min at room temperature and the ECL Prime western blotting detection system (GE Healthcare).

Reverse transcription–polymerase chain reaction

An RNeasy Mini Kit (Qiagen GmbH, Germany) was used in accordance with the manufacturer's instructions to extract total RNA from nonparenchymal cells sorted by fluorescence-activated cell sorting from adult mice treated with DDC. The primers used were as follows: GAPDH (5′-ACCA CAGTCCATGCCATCAC-3′ and 5′-TCCACCACCCTGTTG CTGTA-3′), NS (5′-TCGGAGTCCAGCAAGCATTG-3′ and 5′-GCAGCACTTTCCACATTTGGG-3′), CK19 (5′-GTCCTAC AGATTGACATTGC-3′ and 5′-CACGCTCTGGATCTGTGA CAG-3′), EpCAM (5′-AGGGGCGATCCAGAACAACG-3′ and 5′-ATGGTCGTAGGGGCTTTCTC-3′), Prominin1 (5′-GTA CCTCAGATCCAGCCAGCAA-3′ and 5′-ATTCTTCCAGCT

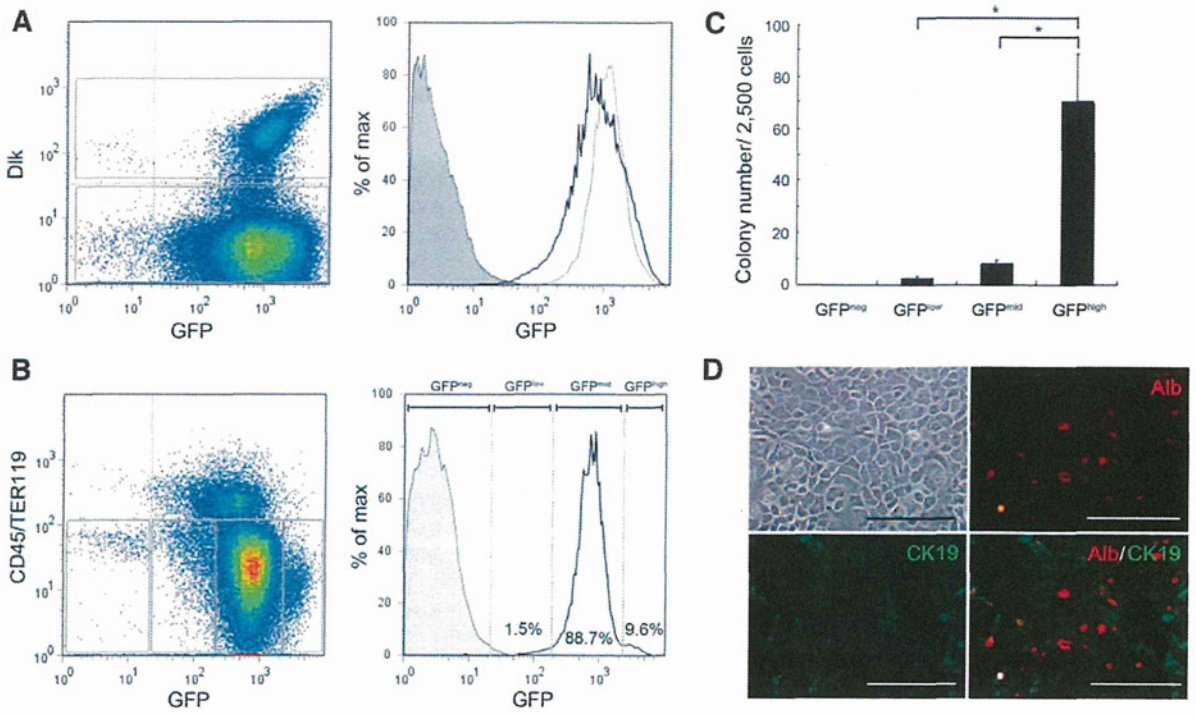

FIG. 1. Correlation of nucleostemin (NS) expression with colony-forming capacity of hepatic precursor cells in developing liver. **(A)** Flow cytometry analysis of green fluorescent protein (GFP) expression in NS-GFP Tg fetal liver. Nonhematopoietic cells from fetal liver cells at E14.5 were isolated by depletion of $CD45^+Ter119^+$ cells. *Left panel*: flow cytometry analysis of Dlk and GFP in $CD45^-Ter119^-$cells. *Right panel*: histogram of GFP expression. GFP expression in Dlk^+ cells (*gray line*) was slightly higher than that seen in Dlk^- cells (*black line*). *Gray region*: wild-type control mouse. The data shown are representative of 3 independent experiments. **(B)** Flow cytometry analysis of GFP expression in NS-GFP Tg neonatal liver. Flow cytometry analysis with CD45/Ter119 and GFP, and histogram with GFP in $CD45^-Ter119^-$ (nonhematopoietic cells) from neonatal liver (P5) are shown in the *left* and *right panels*, respectively. Nonhematopoietic cells ($CD45^-Ter119^-$) were fractionated into GFP^{neg}, GFP^{low}, GFP^{mid}, and GFP^{high} subpopulations. Values in panels are the percentage of the specified subpopulation among $CD45^-Ter119^-$ cells. The data shown are representative of 5 independent experiments. **(C)** Hepatic colony formation of subpopulations in **(B)**. Fractionated cells in **(B)** were cultured for 5 days. Data shown are the mean number ± standard deviation (SD) of colonies ($n = 3$). $^*P < 0.01$ **(D)** Characterization of hepatic colonies. Colonies (brightfield, *upper left panel*) were fixed and stained with anti-albumin (*red*) and anti-CK19 (*green*) antibodies. Most colonies in the culture express albumin or CK19. Representative data are shown. Scale bars, 100 μm.

TGGGCAGC-3′), and CD44 (5′-GGCTTTCAACAGTACC TTAC-3′ and 5′-TGAAGCAATATGTGTCATAG-3′).

Lentiviral transduction of short hairpin RNA

To downregulate NS in hepatic precursor cells or mouse hepatic cell lines (Hepa1-6, a mouse hepatocellular carcinoma cell line and BNL C1. 2, a mouse embryonic liver cell line), lentiviruses carrying short hairpin RNA (shRNA) against NS was prepared as previously described [14]. Oligonucleotides encoding shRNA directed against mouse NS mRNA were synthesized as follows: NS #1: sense, AGTAGA AATTTGATGGGCA; antisense, AGCAGAAACTTGATAG GCA; NS #2: sense, GAGGAAAGTTGTTTCGTTA; antisense, GAAGAAAGTTGTTCCATTA. Hepatic colonies derived from Dlk^+ fetal liver cells or cell lines were infected with lentivirus for 12 h, followed by washes with PBS, and incubation with culture medium. Cell lines were cultured with 10% FCS/DMEM (Invitrogen Life Technologies).

NS knockdown by hydrodynamic shRNA injection

In vivo transfection of shRNA plasmids into hepatocytes was performed by hydrodynamic injection using 6-week-old mice 3 days prior to partial hepatectomy, in accordance with a previous report [20]. A 27-gauge needle was used to inject 40 μg of plasmid in 2 mL PBS through the tail vein within 10 s. Three days later, the animals were sacrificed and the livers were fixed with 4% paraformaldehyde in PBS and embedded in paraffin for sectioning.

Statistical analyses

Statistical differences were determined using the unpaired Student's *t*-test for *P* values.

Results

NS expression correlates with the colony-forming capacity of hepatic precursor cells in developing liver

To investigate NS expression in developing liver, we evaluated GFP intensity in liver cells of NS-GFP Tg fetuses (E14.5) and neonates (P5). Flow cytometry analysis of fetal liver cells showed that most $CD45^-Ter119^-$ (non-hematopoietic) cells expressed high GFP levels (Fig. 1A). Although GFP levels were very high in Dlk^+ cells, in which hepatic stem/precursor cells are enriched [21], those levels were only slightly higher than those in Dlk^- cells (Fig. 1A). Thus, GFP expression was not indicative of a particular subpopulation in fetal liver. Interestingly, however, NS-GFP neonatal liver cells fell into distinct populations based on GFP

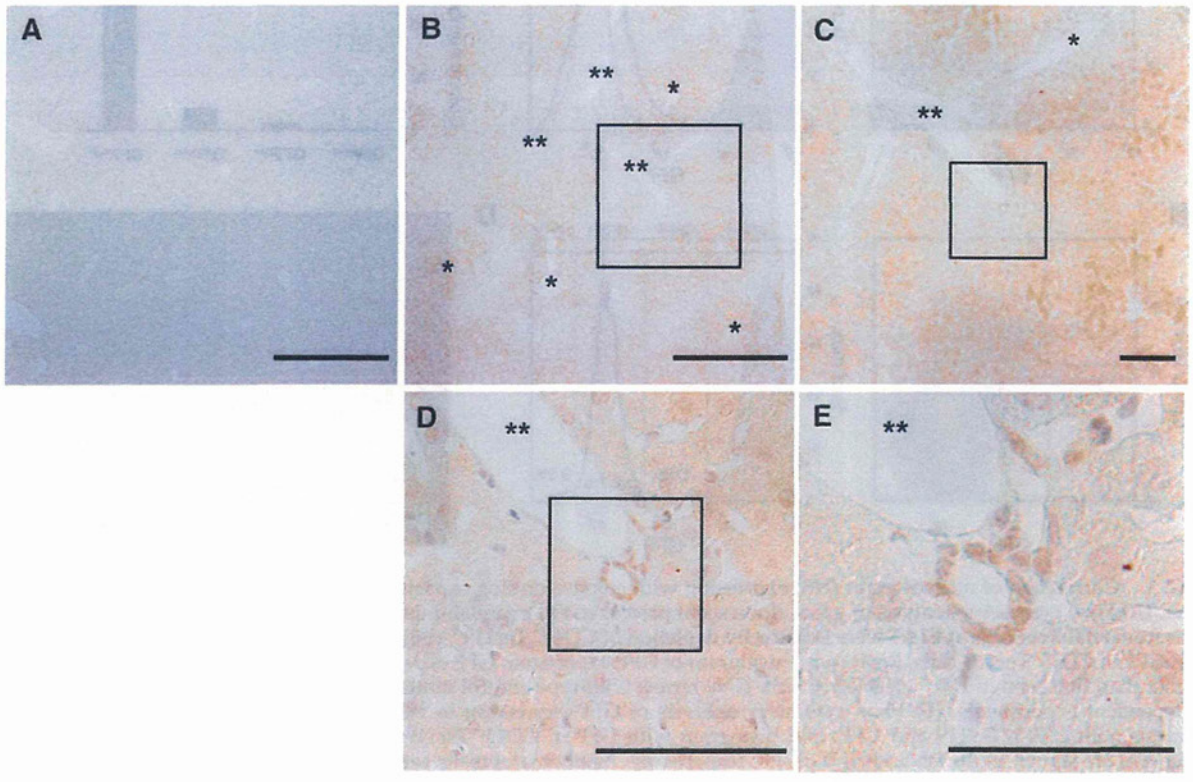

FIG. 2. Expression of NS-GFP in hepatocytes and bile duct epithelial cells of adult liver. **(A–E)** Immunohistochemical analyses of GFP in livers of adult mice (8 weeks old). Sections were stained with an anti-GFP antibody (*brown*), followed by a 3, 3′-diaminobenzidine (DAB) peroxidase reaction. **(A)** Wild-type control (C57BL/6) mice. **(B–E)** NS-GFP Tg mice. **(B)**, **(C)**, and **(D)** are lower-power views of areas shown at higher power in **(C)**, **(D)**, and **(E)**, respectively. Scale bars, 500 μm **(A, B)**, 100 μm **(C, D)**, 50 μm **(E)**, *central vein, **portal vein.

fluorescence intensity (Fig. 1B). While most non-hematopoietic cells were GFP^{mid}, we found a distinct GFP^{high} population. The proportions of GFP^{low} and GFP^{neg} cells were very small. To determine the potential functional significance of these subpopulations, we evaluated hepatic colony forming ability. GFP^{high} cells generated colonies at higher frequency than did any other cell population (Fig. 1C). Most colonies derived from GFP^{high} cells were $CK19^{+}$ or $albumin^{+}$ hepatocytes (Fig. 1D), suggesting that NS is an indicator of hepatic precursor cells in neonatal liver.

Partial hepatectomy upregulates NS expression in hepatocytes

We next examined NS-GFP expression in adult liver. We found that NS-GFP is highly expressed in hepatocytes. In

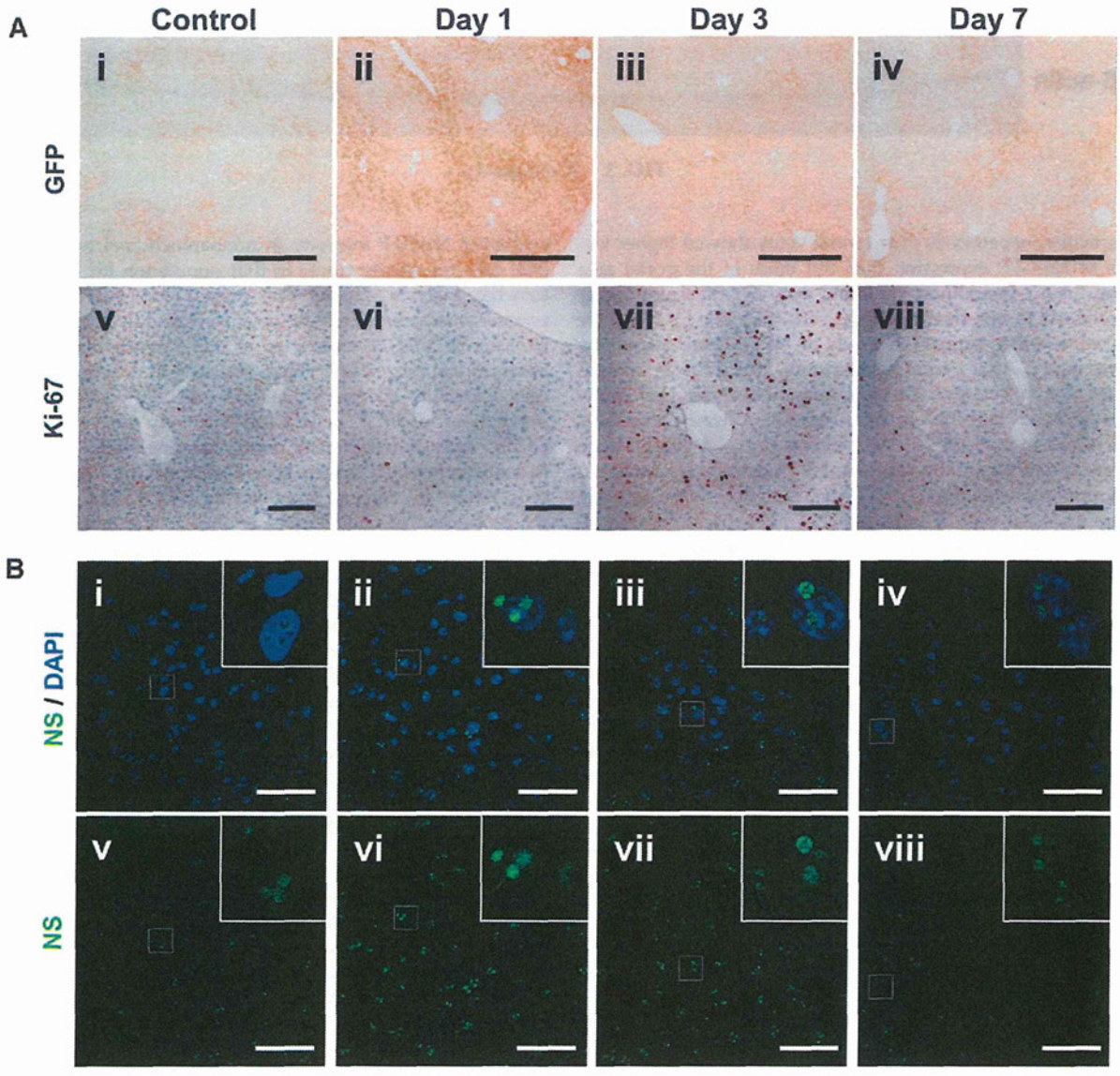

FIG. 3. Upregulation of NS-GFP in adult hepatocytes in response to partial hepatectomy. **(A)** Immunohistochemical analyses of GFP in liver of adult NS-GFP Tg mice after partial hepatectomy. Sections were stained with anti-GFP **(i–iv,** *brown***)** or anti-Ki-67 antibodies **(v–viii,** *brown***)**, followed by DAB peroxidase reactions. **(i, v)** control, **(ii, vi)** day 1, **(iii, vii)** day 3, **(iv, viii)** day 7. Scale bars, 500 μm **(i–iv)**, 100 μm **(v–viii)**. **(B)** Immunohistochemical analyses of endogenous NS in liver of adult NS-GFP Tg mice after partial hepatectomy. Liver sections were stained with an anti-NS antibody, followed by a secondary antibody conjugated to Alexa 488 (*green*, **i–viii)** plus DAPI (nuclear staining, *blue*, **i–iv)**. **(i, v)** control, **(ii, vi)** day 1, **(iii, vii)** day 3, **(iv, viii)** day 7. Scale bars, 50 μm. *Insets* are magnified views of the indicated areas. **(C)** Western blotting analyses of endogenous NS in liver of adult wild-type mice after partial hepatectomy. Lysates were prepared from liver (3 independent samples for each group) and immunoblotted to detect NS and β-actin as a loading control. Short and long exposures are shown for NS in the *upper* and *middle panels*, respectively.

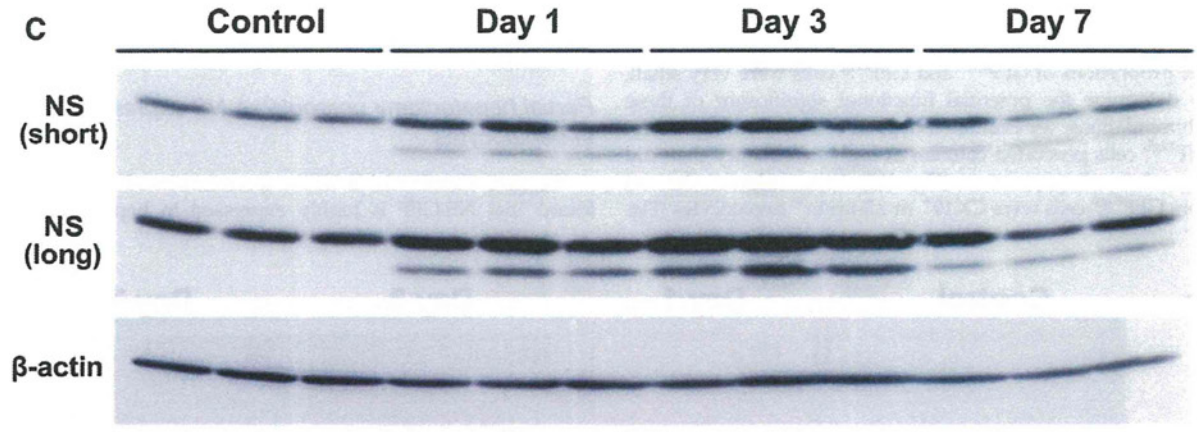

FIG. 3. (Continued).

particular, hepatocytes near central veins showed higher levels of NS-GFP expression than did those in the portal area (Fig. 2A–C). In addition, we found that NS-GFP is also highly expressed in bile duct epithelial cells (Fig. 2D, E). Next, we asked whether expression levels of NS-GFP are altered by liver injury. After partial hepatectomy, NS-GFP was upregulated within 24 h (Fig. 3A i–iv). Immunohistochemical analyses showed that NS protein expression was remarkably increased in nucleoli 24 h after hepatectomy. Although there were variations among samples, NS protein levels appeared to remain elevated at day 3 (Fig. 3B) and reverted to baseline levels at day 7, whereas NS-GFP expression was already downregulated at day 3. Western blotting analysis using an anti-NS antibody consistently showed an increase in endogenous NS protein on day 1 and day 3 after partial hepatectomy (Fig. 3C). The discrepancy between NS-GFP and endogenous NS is possibly due to differences in protein stability stemming from different post-translational modification of these molecules. Interestingly, partial hepatectomy induced a variant form of NS that is reported to be expressed in particular tissues [22,23]. Hepatocytes that had begun to proliferate showed a small increase in the expression of Ki-67, a marker of cell proliferation, at day 1, and further increases in Ki-67 expression were observed at day 3 (Fig. 3A v–viii). These data indicate that NS gene expression is rapidly upregulated before the start of cell division in response to partial hepatectomy.

A DDC diet induces emergence of ductal epithelial cells expressing NS-GFP

DDC treatment inhibits the capacity for hepatocytes to regenerate, while inducing ductal proliferation in mice in what is known as the oval cell response [6]. We found that DDC treatment reduced expression of NS-GFP in hepatocytes (Fig. 4A i, ii) compared to the expression in untreated hepatocytes. We also found that bile duct-like NS-GFP-positive cells emerged in the portal zone following DDC treatment (Fig. 4A iii, iv). Interstitial cells surrounding ductal cells did not express NS-GFP. We confirmed by immunofluorescence that NS-GFP was expressed in $CK19^+$ ductal epithelial cells (Fig. 4B). To investigate the regenerative capacity of NS-GFP-expressing cells in DDC-treated liver, we evaluated NS-GFP intensity in nonparenchymal cells, since oval cells reportedly reside in that population [6]. Flow cytometry analysis showed that most $CD45^-Ter119^-$ nonparenchymal cells were GFP-positive (Fig. 5A), although the intensity of NS-GFP expression in non-parenchymal cells in adult mice appeared lower than that seen in developing liver cells. These NS-GFP-positive cells fell into GFP^{high} and GFP^{low} populations. GFP^{high} cells were relatively rare, but only GFP^{high} cells showed hepatic colony forming ability (Fig. 5C). In contrast, no colonies were generated from GFP^{low} or GFP^{neg} cells. Severe liver injury promoted by a DDC diet increased the proportion of GFP^{high} cells relative to the proportion in untreated mice (Fig. 5B). Because we found that ductal cells express NS-GFP (Figs. 2 and 4), we assumed that the DDC diet increased the number of ductal cells, resulting in an increase in the proportion of GFP^{high} cells. Hepatic colonies were generated only from GFP^{high} cells (Fig. 5D). GFP^{high} cells expressed higher levels of NS mRNA, indicating that GFP expression corresponded with that of endogenous NS, and also expressed several genes reportedly expressed in oval cells [19] (Fig. 5E). These data indicate that hepatic precursor cells induced by severe liver injury express NS.

NS downregulation inhibits proliferation of hepatic precursor cells

Next, to address whether NS is required for regeneration of hepatic precursor cells, we downregulated NS expression in hepatic cell line and primary fetal liver cells in vitro. Previously, we successfully suppressed NS in a germ cell line by infection with a lentivirus carrying NS shRNA [14]. In this system, infected cells were identified by GFP expression driven by the lentivirus vector (GFP^+ cells). For the current study, we infected the mouse hepatocellular carcinoma cell line Hepa1-6 and the mouse embryonic liver cell line BNL C1.2 with lentiviruses carrying NS shRNA (#1 or #2) or a scrambled control shRNA and then stained the cells with an anti-NS antibody. Both shRNAs, but not the scrambled control, efficiently reduced expression of NS protein in the hepatic cell lines (Fig. 6A, data not shown). NS knockdown (GFP^+) cells in the cell lines had dramatically reduced colony-forming capacity (Fig. 6B, data not shown). We also found that NS downregulation significantly decreased the

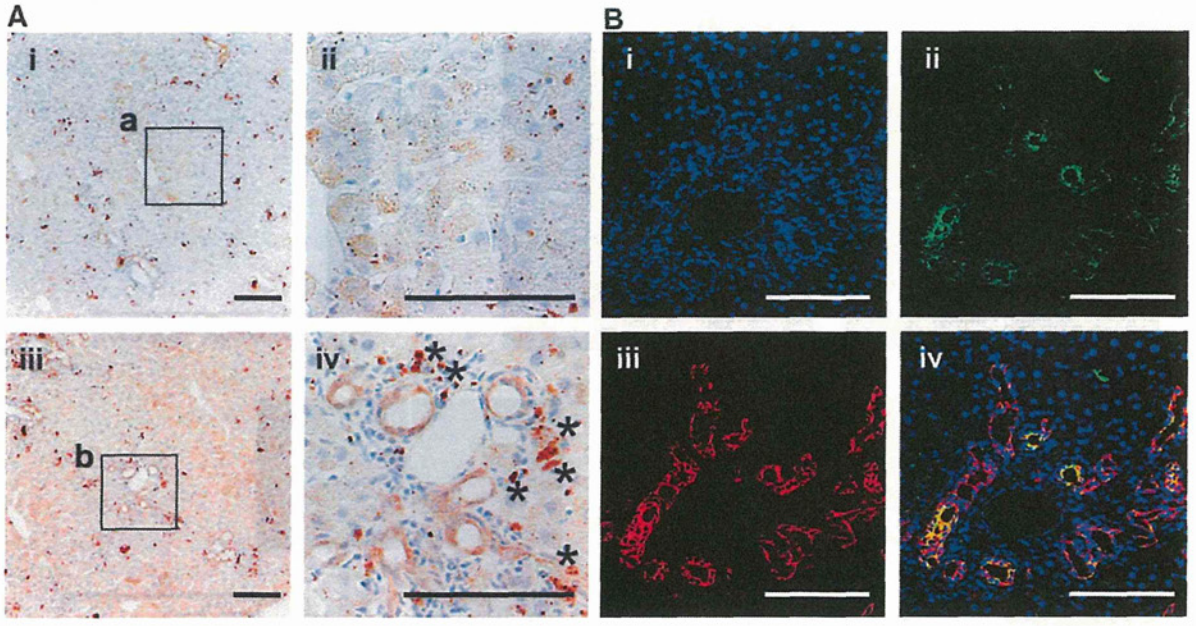

FIG. 4. Duct-like cells express NS-GFP in liver of adult mice fed a 3,5-diethoxycarbonyl-1,4-dihydrocollidine (DDC) diet. **(A, B)** GFP in hepatocytes of adult NS-GFP Tg mice fed a DDC diet. **(A)** Sections were stained with an anti-GFP antibody. **a** and **b** are lower power views of the areas shown at higher power in **(ii)** and **(iv)**, respectively. *Deposition of iron hemes, visible as *brown* clots. **(B)** Sections were stained with anti-GFP (*green*) and anti-CK19 (*red*) antibodies and DAPI (nuclear staining, *blue*). **(i)** DAPI, **(ii)** GFP, **(iii)** CK19, **(iv)** merged. Scale bars, 100 μm.

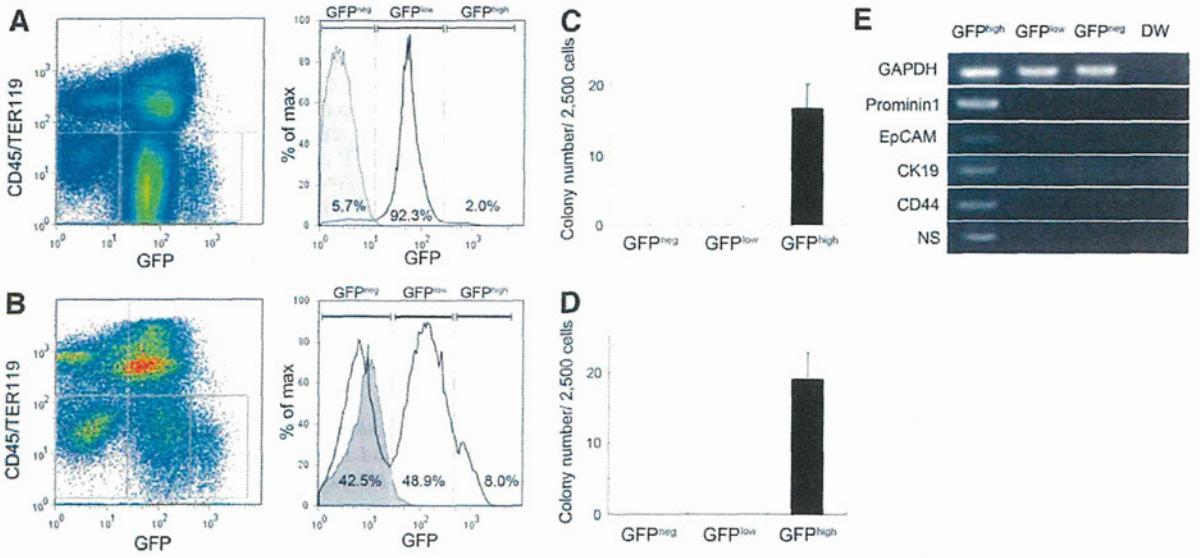

FIG. 5. Increased ratios of NS-GFP^{high} hepatic precursor cells are seen following a DDC diet. **(A, B)** Flow cytometric analyses of GFP expression in nonparenchymal cells of adult NS-GFP Tg mice without **(A)** and with **(B)** a DDC diet. Flow cytometry with CD45/Ter119 and GFP, and a histogram of GFP in CD45$^-$Ter119$^-$ cells are shown in the *left* and *right* panels, respectively. Nonhematopoietic nonparenchymal cells (CD45$^-$Ter119$^-$) were fractionated into 3 distinct subpopulations (GFP^{neg}, GFP^{low}, and GFP^{high} cells). Values in panels are the percentage of the specified subpopulation among CD45$^-$ Ter119$^-$ cells. The data shown are representative of 3 independent experiments. **(C, D)** Hepatic colony formation of subpopulations. Fractionated cells were cultured for 7 days. Data shown are the mean ratio ± SD of colonies derived from mice fed a control **(C)** and DDC **(D)** diet ($n = 3$ each). **(E)** Gene expression in NS-GFP subpopulations. Total RNA was purified from the subpopulations indicated in **(B)**, and mRNA levels of the indicated molecules were evaluated by reverse transcription–polymerase chain reaction. DW, distilled water.

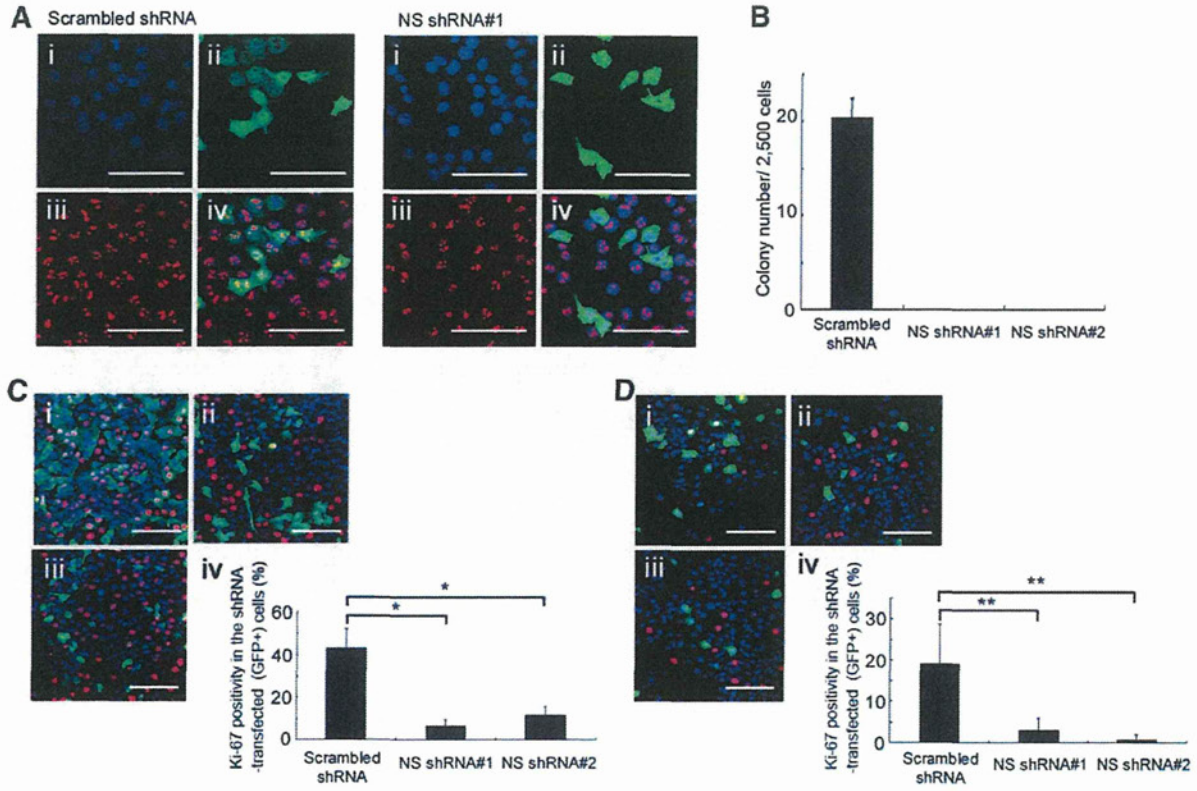

FIG. 6. Inhibition of proliferation of hepatic precursor cells following NS downregulation in vitro. **(A)** NS knockdown in a hepatic cell line. A scrambled shRNA (control, *left panels*) or NS shRNA#1 (*right panels*) was introduced into Hepa1-6 cells (a murine hepatocellular carcinoma cell line) by lentiviral infection, followed by staining with anti-GFP (*green*) and anti-NS (*red*) antibodies and DAPI (*blue*). **(i)** DAPI, **(ii)** GFP, **(iii)** NS, **(iv)** merged. NS protein expression (*red*) was reduced in GFP^+ cells treated with shRNA#1 but not the control shRNA. **(B)** Colony formation of Hepa1-6 cells following NS knockdown. GFP^+ Hepa1-6 cells, indicating those transduced with shRNA, were isolated and cultured for 10 days. Data shown are the mean number ± SD of colonies ($n = 3$). **(C, D)** Proliferation of Hepa1-6 cells **(C)** and Dlk^+ hepatic precursors from fetal liver **(D)** following NS knockdown. Hepa1-6 cells and Dlk^+ fetal liver cells were infected with the shRNA lentivirus, and then cultured for 3 **(C)** or 10 **(D)** days. Cells were stained with an anti-Ki-67 antibody (*red*), anti-GFP antibody (*green*), and DAPI (*blue*). Representative data are shown in **(i)**, **(ii)**, and **(iii)** for the scrambled control, NS shRNA#1, and NS shRNA#2, respectively. Data shown in **(iv)** are the mean ratio ± SD of Ki-67 positivity among cells transfected with the indicated shRNA plasmids (GFP^+ cells) ($n = 3$).*$P < 0.01$, **$P < 0.05$. Scale bars, 100 μm.

proportion of Ki-67-positive cells among transfected (GFP^+) cells in the hepatic cell line (Fig. 6C) and in the hepatic colonies derived from freshly isolated fetal liver precursor cells (Fig. 6D). Thus, NS downregulation inhibits proliferation of hepatic precursor cells.

NS plays an essential role in hepatocyte proliferation in response to liver injury in vivo

The observation that NS is upregulated in hepatocytes after partial hepatectomy suggested that NS is essential for hepatocyte proliferation. To examine the effect of loss NS function in hepatocytes in vivo, we introduced the shRNA plasmids into liver cells by hydrodynamic injection of plasmid DNA via the tail vein [20]. Partial hepatectomy was performed 3 days later and we found that hepatocytes were successfully transfected with shRNA plasmids by detection of GFP expression. Three days after partial hepatectomy, we found that NS knockdown in the hepatocytes significantly suppressed expression of the Ki-67 antigen (Fig. 7), indicating that NS is essential for hepatocyte proliferation in response to liver injury in vivo.

Discussion

In this study, we examined the expression and function of NS in developing and injured liver, and we evaluated the capacity of hepatic NS-expressing cells to form colonies by using an NS-GFP system. As previously reported [19], DDC treatment induced the emergence of ductal cells that express both cholangiocellular and hepatocytic markers, called "oval cells," in periportal regions. Several studies have identified markers of oval cells, including Ep-CAM and CD133 [19,24,25]. NS-GFP was not specific for oval cells, since most hepatocytes and nonparenchymal cells also expressed GFP. Therefore, NS-GFP expression alone cannot be used to purify hepatic stem/precursor cells. However, since a distinct subpopulation of cells expressing high GFP levels (GFP^{high}) showed higher clonogenic potential, combining this system with evaluation of other stem cell markers could enable

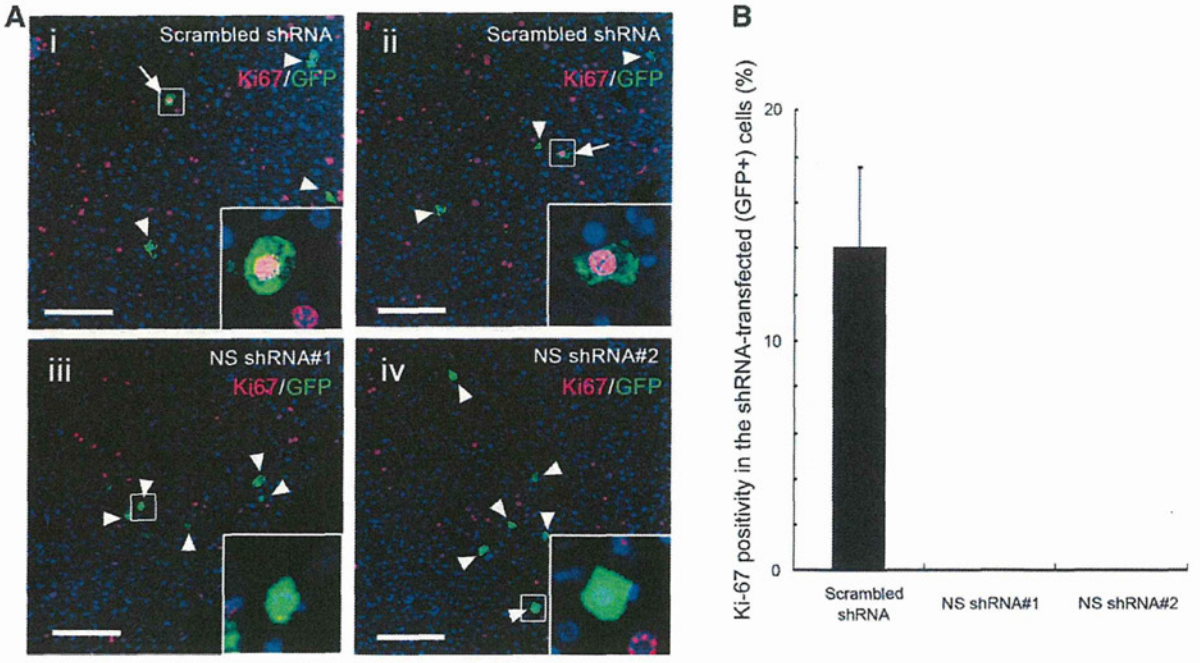

FIG. 7. Inhibition of hepatocyte proliferation following NS downregulation in vivo. NS shRNA plasmids were introduced into liver cells by hydrodynamic injection of the plasmid DNA via the tail vein, followed by partial hepatectomy 3 days after injection. Liver tissue specimens were prepared 3 days later, and sections were stained with an anti-GFP antibody (*green*), anti-Ki-67 antibody (*red*), and DAPI (*blue*). Ki-67 expression was evaluated in more than 60 GFP^+ cells for each sample. **(A)** Representative data for the scrambled control **(i, ii)**, NS shRNA#1 **(iii)**, and NS shRNA#2 **(iv)**. *Arrows*; $GFP^+Ki\text{-}67^+$ cells, *arrowheads*; $GFP^+Ki\text{-}67^-$cells. *Insets* are magnified views of the indicated areas. **(B)** Mean percentage ± SD of Ki-67 positivity in hepatocytes transfected with the indicated shRNA plasmids (GFP^+ cells) ($n=3$). Scale bars, 100 μm.

efficient enrichment of a stem/precursor cell population. In addition, NS may be particularly important for the development of liver, since the expression level of NS-GFP in developing liver cells appeared to be higher than that in adult non-parenchymal cells. NS may therefore play a critical role in expansion of the hepatic stem/precursor cells during liver development.

A previous study demonstrated that NS is required for rRNA processing [9,26], suggesting that NS expression regulates protein synthesis. Enhanced protein synthesis requires activation of ribosomal biogenesis. NS belongs to the class of nucleolar GTPases that includes yeast Nug1, which exports pre-60S ribosomal subunits out of the nucleolus [27]. In *Caenorhabditis elegans*, *nst-1* mutants exhibit reduced rRNA levels, suggesting a critical role of NS in ribosome biogenesis [9]. NS knockdown apparently delays processing of 32S pre-rRNA into 28S rRNA and is accompanied by a substantial decrease in protein synthesis and in the levels of rRNAs and some mRNAs [26]. Because protein synthesis is required for cell growth and proliferation, NS expression in both hepatic precursor cells and hepatocytes may be important for tissue regeneration. On the other hand, protein synthesis appears to be enhanced in resting hepatocytes for reasons unrelated to regeneration. Mature hepatocytes exhibit high levels of protein synthesis to maintain serum protein levels, and protein translation actively occurs even in non-dividing hepatocytes. Thus, NS expression may be controlled by several different signals.

One possible regulator of NS is Myc, which is upregulated by partial hepatectomy [28]. When Myc is overexpressed in mouse hepatocytes in vivo using recombinant adenovirus, hepatocytes enlarge in the absence of significant cell proliferation, an event associated with upregulation of large- and small-subunit ribosomal and nucleolar genes [29]. In addition, a recent study identified the NS gene as a direct transcriptional target of the Myc oncoprotein [22]. Therefore, NS may function to increase cell mass in response to Myc activation following partial hepatectomy. It has also been reported that, constitutive activation of Myc generates hepatocellular carcinoma, whereas Myc inactivation promotes differentiation of tumor cells into hepatocytes and biliary cells, which form bile duct structures [30], suggesting that Myc maintains cells in an undifferentiated status. NS may have a similar function in the case of hepatic malignancy. In addition, Myc may control post-translational regulation of NS protein. A recent study revealed that NS is a target of reactive oxygen species (ROS) [31]. In transformed hematopoietic cells, Myc activation leads to high ROS levels, resulting in impaired NS protein degradation. Therefore, Myc activation may stabilize NS protein in regenerating liver. Because GFP would not be stabilized in the same way as the NS protein, these findings suggest that NS protein levels may not be precisely correlated with NS-GFP levels. Nonetheless, both NS protein levels and NS-GFP expression are consistently upregulated by partial hepatectomy. These findings suggest that overall NS expression is likely regulated by both transcriptional and protein stability.

In conclusion, we have demonstrated that NS is essential for proliferation of both hepatic precursor cells and

hepatocytes. Understanding the mechanisms regulating NS expression and function may contribute to development of methodologies useful for enhancing liver regeneration in pathological states.

Acknowledgments

We thank Drs. Akihide Kamiya, Hiromitsu Nakauchi, Tetsuhiro Chiba, Atsushi Iwama, and Atsushi Miyajima for providing information and technical advice for establishing assay systems for hepatic colony formation and isolation of liver cells and Dr. Kenichi Harada for insightful suggestions for histological analyses. A.H. was supported by a Grant-in-Aid for Scientific Research on Innovative Areas and the Project for Development of Innovative Research on Cancer Therapeutics (P-DIRECT) from the Ministry of Education, Culture, Sports, Science and Technology, Japan, and by a grant from the Japan Science and Technology Agency (JST), CREST.

Author Disclosure Statement

No competing financial interests exist.

References

1. Michalopoulos GK and MC DeFrances. (1997). Liver regeneration. Science 276:60–66.
2. Michalopoulos GK. (2010). Liver regeneration after partial hepatectomy: critical analysis of mechanistic dilemmas. Am J Pathol 176:2–13.
3. Tanaka M, T Itoh, N Tanimizu and A Miyajima. (2011). Liver stem/progenitor cells: their characteristics and regulatory mechanisms. J Biochem 149:231–239.
4. Oertel M and DA Shafritz. (2008). Stem cells, cell transplantation and liver repopulation. Biochim Biophys Acta 1782:61–74.
5. Farber E. (1956). Similarities in the sequence of early histological changes induced in the liver of the rat by ethionine, 2-acetylamino-fluorene, and 3'-methyl-4-dimethylaminoazobenzene. Cancer Res 16:142–148.
6. Preisegger KH, VM Factor, A Fuchsbichler, C Stumptner, H Denk and SS Thorgeirsson. (1999). Atypical ductular proliferation and its inhibition by transforming growth factor beta1 in the 3,5-diethoxycarbonyl-1,4-dihydrocollidine mouse model for chronic alcoholic liver disease. Lab Invest 79:103–109.
7. Tsai RY and RD McKay. (2002). A nucleolar mechanism controlling cell proliferation in stem cells and cancer cells. Genes Dev 16:2991–3003.
8. Nomura J, M Maruyama, M Katano, H Kato, J Zhang, S Masui, Y Mizuno, Y Okazaki, M Nishimoto and A Okuda. (2009). Differential requirement for nucleostemin in embryonic stem cell and neural stem cell viability. Stem Cells 27:1066–1076.
9. Kudron MM and V Reinke. (2008). *C. elegans* nucleostemin is required for larval growth and germline stem cell division. PLoS Genet 4:e1000181.
10. Maki N, K Takechi, S Sano, H Tarui, Y Sasai and K Agata. (2007). Rapid accumulation of nucleostemin in nucleolus during newt regeneration. Dev Dyn 236:941–950.
11. Beekman C, M Nichane, S De Clercq, M Maetens, T Floss, W Wurst, E Bellefroid and JC Marine. (2006). Evolutionarily conserved role of nucleostemin: controlling proliferation of stem/progenitor cells during early vertebrate development. Mol Cell Biol 26:9291–9301.
12. Han C, X Zhang, W Xu, W Wang, H Qian and Y Chen. (2005). Cloning of the nucleostemin gene and its function in transforming human embryonic bone marrow mesenchymal stem cells into F6 tumor cells. Int J Mol Med 16: 205–213.
13. Hirai H, L Romanova, S Kellner, M Verma, S Rayner, A Asakura and N Kikyo. (2010). Post-mitotic role of nucleostemin as a promoter of skeletal muscle cell differentiation. Biochem Biophys Res Commun 391:299–304.
14. Ohmura M, K Naka, T Hoshii, T Muraguchi, H Shugo, A Tamase, N Uema, T Ooshio, F Arai, et al. (2008). Identification of stem cells during prepubertal spermatogenesis via monitoring of nucleostemin promoter activity. Stem Cells 26:3237–3246.
15. Tamase A, T Muraguchi, K Naka, S Tanaka, M Kinoshita, T Hoshii, M Ohmura, H Shugo, T Ooshio, et al. (2009). Identification of tumor-initiating cells in a highly aggressive brain tumor using promoter activity of nucleostemin. Proc Natl Acad Sci U S A 106:17163–17168.
16. Lin T, L Meng, Y Li and RY Tsai. (2010). Tumor-initiating function of nucleostemin-enriched mammary tumor cells. Cancer Res 70:9444–9452.
17. Okamoto N, M Yasukawa, C Nguyen, V Kasim, Y Maida, R Possemato, T Shibata, KL Ligon, K Fukami, WC Hahn and K Masutomi. (2011). Telomerase and retrotransposons: reverse transcriptases that shaped genomes special feature sackler colloquium: maintenance of tumor initiating cells of defined genetic composition by nucleostemin. Proc Natl Acad Sci U S A 108:20388–20393.
18. Kamiya A, T Kinoshita, Y Ito, T Matsui, Y Morikawa, E Senba, K Nakashima, T Taga, K Yoshida, T Kishimoto and A Miyajima. (1999). Fetal liver development requires a paracrine action of oncostatin M through the gp130 signal transducer. EMBO J 18:2127–2136.
19. Okabe M, Y Tsukahara, M Tanaka, K Suzuki, S Saito, Y Kamiya, T Tsujimura, K Nakamura and A Miyajima. (2009). Potential hepatic stem cells reside in EpCAM+ cells of normal and injured mouse liver. Development 136: 1951–1960.
20. Zhang G, V Budker and JA Wolff. (1999). High levels of foreign gene expression in hepatocytes after tail vein injections of naked plasmid DNA. Hum Gene Ther 10:1735–1737.
21. Tanimizu N, M Nishikawa, H Saito, T Tsujimura and A Miyajima. (2003). Isolation of hepatoblasts based on the expression of Dlk/Pref-1. J Cell Sci 116:1775–1786.
22. Zwolinska AK, A Heagle Whiting, C Beekman, JM Sedivy and JC Marine. (2011). Suppression of Myc oncogenic activity by nucleostemin haploinsufficiency. Oncogene 2011 [Epub ahead of print]; DOI: 10.1038/onc.2011.507.
23. Malakootian M, SJ Mowla, H Saberi, MH Asadi, Y Atlasi and AM Shafaroudi. (2010). Differential expression of nucleostemin, a stem cell marker, and its variants in different types of brain tumors. Mol Carcinog 49:818–825.
24. Suzuki A, S Sekiya, M Onishi, N Oshima, H Kiyonari, H Nakauchi and H Taniguchi. (2008). Flow cytometric isolation and clonal identification of self-renewing bipotent hepatic progenitor cells in adult mouse liver. Hepatology 48:1964–1978.
25. Kamiya A, S Kakinuma, Y Yamazaki and H Nakauchi. (2009). Enrichment and clonal culture of progenitor cells during mouse postnatal liver development in mice. Gastroenterology 137:1114–1126.

26. Romanova L, A Grand, L Zhang, S Rayner, N Katoku-Kikyo, S Kellner and N Kikyo. (2009). Critical role of nucleostemin in pre-rRNA processing. J Biol Chem 284:4968–4977.
27. Bassler J, P Grandi, O Gadal, T Lessmann, E Petfalski, D Tollervey, J Lechner and E Hurt. (2001). Identification of a 60S preribosomal particle that is closely linked to nuclear export. Mol Cell 8:517–529.
28. Morello D, MJ Fitzgerald, C Babinet and N Fausto. (1990). c-myc, c-fos, and c-jun regulation in the regenerating livers of normal and H-2K/c-myc transgenic mice. Mol Cell Biol 10:3185–3193.
29. Kim S, Q Li, CV Dang and LA Lee. (2000). Induction of ribosomal genes and hepatocyte hypertrophy by adenovirus-mediated expression of c-Myc *in vivo*. Proc Natl Acad Sci U S A 97:11198–11202.
30. Shachaf CM, AM Kopelman, C Arvanitis, A Karlsson, S Beer, S Mandl, MH Bachmann, AD Borowsky, B Ruebner, et al. (2004). MYC inactivation uncovers pluripotent differentiation and tumour dormancy in hepatocellular cancer. Nature 431:1112–1117.
31. Huang M, P Whang, JV Chodaparambil, DA Pollyea, B Kusler, L Xu, DW Felsher and BS Mitchell. (2011). Reactive oxygen species regulate nucleostemin oligomerization and protein degradation. J Biol Chem 286:11035–11046.

Address correspondence to:
Dr. Atsushi Hirao
Division of Molecular Genetics
Cancer Research Institute
Kanazawa University
Kakuma-machi
Kanazawa, Ishikawa 920-1192
Japan

E-mail: ahirao@staff.kanazawa-u.ac.jp

Received for publication December 25, 2011
Accepted after revision May 10, 2012
Prepublished on Liebert Instant Online July 9, 2012

Published OnlineFirst May 31, 2012; DOI:10.1158/0008-5472.CAN-12-0028

Therapeutics, Targets, and Chemical Biology

Cancer Research

Acyclic Retinoid Targets Platelet-Derived Growth Factor Signaling in the Prevention of Hepatic Fibrosis and Hepatocellular Carcinoma Development

Hikari Okada[1], Masao Honda[1,2], Jean S. Campbell[4], Yoshio Sakai[1], Taro Yamashita[1], Yuuki Takebuchi[1], Kazuhiro Hada[1], Takayoshi Shirasaki[1], Riuta Takabatake[1], Mikiko Nakamura[1], Hajime Sunagozaka[1], Takuji Tanaka[3], Nelson Fausto[4], and Shuichi Kaneko[1]

Abstract

Hepatocellular carcinoma (HCC) often develops in association with liver cirrhosis, and its high recurrence rate leads to poor patient prognosis. Although recent evidence suggests that peretinoin, a member of the acyclic retinoid family, may be an effective chemopreventive drug for HCC, published data about its effects on hepatic mesenchymal cells, such as stellate cells and endothelial cells, remain limited. Using a mouse model in which platelet-derived growth factor (PDGF)-C is overexpressed (*Pdgf-c Tg*), resulting in hepatic fibrosis, steatosis, and eventually, HCC development, we show that peretinoin significantly represses the development of hepatic fibrosis and tumors. Peretinoin inhibited the signaling pathways of fibrogenesis, angiogenesis, and Wnt/β-catenin in *Pdgf-c* transgenic mice. *In vitro*, peretinoin repressed the expression of PDGF receptors α/β in primary mouse hepatic stellate cells (HSC), hepatoma cells, fibroblasts, and endothelial cells. Peretinoin also inhibited PDGF-C–activated transformation of HSCs into myofibroblasts. Together, our findings show that PDGF signaling is a target of peretinoin in preventing the development of hepatic fibrosis and HCC. *Cancer Res; 72(17); 4459–71. ©2012 AACR.*

Introduction

Hepatocellular carcinoma (HCC) is one of the most common malignancies worldwide with a particularly poor patient outcome (1). It often develops as a result of chronic liver disease associated with hepatitis B or hepatitis C virus infection or with other etiologies such as long-term alcohol abuse, autoimmunity, and hemochromatosis (2–5). Despite the recent advances in antiviral therapy for hepatitis B or hepatitis C virus, these are insufficient to completely prevent the occurrence of HCC. Moreover, the recent increase in nonalcoholic fatty liver disease (NAFLD) associated with metabolic syndrome is a potential high-risk factor for the development of HCC (6).

HCC often develops during the advanced stages of liver fibrosis and is associated with deposits of extracellular matrix synthesized by activated stellate cells. During the course of chronic hepatitis, nonparenchymal cells, including Kupffer, endothelial, and activated stellate cells, release a variety of cytokines and growth factors. One of these growth factors is platelet-derived growth factor (PDGF), which is involved in fibrogenesis, angiogenesis, and tumorigenesis (7, 8). PDGF expression has been shown to be upregulated from the early stages of chronic hepatitis, suggesting its association with the development of fibrosis in chronic hepatitis C (CH-C; refs. 9 and 10). Overexpression of PDGF-C in mouse liver resulted in the progression of hepatic fibrosis, steatosis, and the development of HCC; this mouse model closely resembles the human HCC, which is frequently associated with hepatic fibrosis (7).

Peretinoin (generic name; code, NIK-333), developed by the Kowa Company, is an oral acyclic retinoid with a vitamin A–like structure, which targets the retinoid nuclear receptor. Oral administration of peretinoin was shown to significantly reduce the incidence of posttherapeutic HCC recurrence and improve the survival rates of patients in a clinical trial (11, 12). A large-scale clinical study including various countries is now planned to confirm its clinical efficacy.

Although peretinoin treatment can suppress HCC-derived cell line growth and inhibit experimental mouse or rat liver carcinogenesis (13, 14), the detailed mechanism of its effect has not been fully elucidated. Peretinoin has a high binding affinity to cellular retinoic acid-binding protein (15) and may interact with retinoic acid receptor-β and retinoid X receptor-α (16); however, the precise molecular targets for preventing HCC recurrence have not yet been elucidated.

Authors' Affiliations: [1]Department of Gastroenterology, Kanazawa University Graduate School of Medicine; [2]Department of Advanced Medical Technology, Kanazawa University Graduate School of Health Medicine; [3]Department of Oncologic Pathology, Kanazawa Medical University, Kanazawa, Japan; and [4]Department of Pathology, University of Washington School of Medicine, Seattle, Washington

Note: Supplementary data for this article are available at Cancer Research Online (http://cancerres.aacrjournals.org/).

Corresponding Author: Masao Honda, Department of Gastroenterology, Graduate School of Medicine, Kanazawa University, Takara-Machi 13-1, Kanazawa 920-8641, Japan. Phone: 81-76-265-2235; Fax: 81-76-234-4250; E-mail: mhonda@m-kanazawa.jp

doi: 10.1158/0008-5472.CAN-12-0028

Published OnlineFirst May 31, 2012; DOI:10.1158/0008-5472.CAN-12-0028

In this study, we used PDGF-C transgenic (*Pdgf-c* Tg) mice to show that PDGF-C signaling is a possible target of peretinoin in the prevention of hepatic fibrosis, angiogenesis, and the development of HCC.

Materials and Methods

Chemicals

The acyclic retinoid peretinoin (generic name; code, NIK-333) [(2E,4E,6E,10E)-3,7,11,15-tetramethyl-2,4,6,10,14-hexadecapentaenoic acid, C20H30O2, molecular weight 302.46 g/mol] was supplied by Kowa Company.

Animal studies

The generation and characterization of *Pdgf-c Tg* have been described previously (7). Wild-type and *Pdgf-c Tg* mice on a C57BL/6J background were maintained in a pathogen-free animal facility under a standard 12-hour/12-hour light/dark cycle. After weaning at week 4, male mice were randomly divided into the following 3 groups: (1) *Pdgf-c Tg* or wild-type (WT) mice given a basal diet (CRF-1, Charles River Laboratories Japan), (2) *Pdgf-c Tg* or WT mice given a 0.03% peretinoin-containing diet, (3) *Pdgf-c Tg* or WT mice given a 0.06% peretinoin-containing diet. Control mice were normal male homozygotes. At week 20, mice were sacrificed to analyze the progression of hepatic fibrosis ($n = 15$ for each of the 3 groups). At week 48, mice were sacrificed to analyze the development of hepatic tumors ($n = 31$ for the basal diet group, $n = 37$ for the 0.03% peretinoin group, and $n = 17$ for the 0.06% peretinoin group). The incidence of hepatic tumors, maximum tumor size, and liver weight were evaluated. None of the treated WT mice given a diet of 0.03% peretinoin died, but death occurred in 5% of WT mice around after 36 weeks of age receiving a 0.06% peretinoin diet, probably because of its toxicity. In *Pdgf-c Tg* mice, death was observed at similar frequency as WT mice that received 0.06% peretinoin diet.

All animal experiments were carried out in accordance with Guidelines for the Care and Use of Laboratory Animals at the Takara-Machi Campus of Kanazawa University, Japan.

Cell culture

Human HCC cell lines Huh-7, HepG2, and HLE, the mouse fibroblast cell line NIH3T3, human umbilical vein endothelial cells (HUVEC), and human stellate cells Lx-2 (kindly provided by Dr. Scott Friedman, Mount Sinai School of Medicine, New York, NY) were maintained in Dulbecco's Modified Eagle Medium (DMEM; Gibco) supplemented with 10% FBS (Gibco), 1% L-glutamine (Gibco), and 1% penicillin/streptomycin (Gibco) in a humidified atmosphere of 5% CO_2 at 37°C. 1 to 5×10^4 cells were seeded in each well of a 12-well plate the day before serum starvation in serum-free DMEM for 8 hours. The culture medium was then replaced with serum-free medium containing peretinoin. After 24-hour incubation, cells were harvested for analysis.

Isolation and culture of mouse hepatic stellate cells

Hepatic stellate cells (HSC) were isolated from C57BL/6J mice and the effect of recombinant human PDGF-C and peretinoin on HSCs was evaluated *in vitro*. Pronase-collagenase liver digestion was used to isolate HSC from wild-type mice. All experiments were replicated at least twice. Freshly isolated HSCs suspended in culture medium were seeded in uncoated 24-well plates and incubated at 37°C in a humidified atmosphere of 5% CO_2 for 72 hours. Nonadherent cells were removed with a pipette and the culture medium was replaced with medium containing 80 ng/mL recombinant human PDGF-C (Abnova) with or without peretinoin or 9-*cis*-retinoic acid (9cRA; 5 or 10 μmol/L). Cells were harvested for analysis after 24-hour incubation.

Isolation of peripheral blood mononuclear cells

Peripheral blood mononuclear cells were harvested and labeled with FITC-conjugate CD34 (Cell Lab) and R-Phycoerythrin (PE)-conjugated CD31 antibodies (Cell Lab) for 30 minutes at 4°C. After washing with 1 mL PBS, CD31 and CD34 surface expression was measured with a FACSCalibur flow cytometer (BD Biosciences). All flow cytometric data were analyzed using FlowJo software (Tree Star).

Gene expression profiling

Gene expression profiling in mouse liver was evaluated using the GeneChip Mouse Genome 430 2.0 Array (Affymetrix). Liver tissue from WT, *Pdgf-c Tg*, and *Pdgf-c Tg* with 0.06% peretinoin mice all at weeks 20 and 48 was obtained and a total of 34 chip assays were conducted as described previously (17). Expression data have been deposited in the Gene Expression Omnibus (GEO; NCBI Accession; GSE31431).

Pathway analysis was conducted using MetaCore (GeneGo). Functional ontology enrichment analysis was conducted to compare the Gene Ontology (GO) process distribution of differentially expressed genes ($P < 0.01$; refs. 10 and 17). Direct interactions among differentially expressed genes between *Pdgf-c Tg* mice with or without peretinoin administration were examined as reported previously (10). Each connection represents a direct, experimentally confirmed, physical interaction (MetaCore).

Histopathology and immunohistochemical staining

Mouse liver tissues were fixed in 10% formalin and stained with hematoxylin and eosin. The liver neoplasms (HCC and liver cell adenoma) were diagnosed according to previously described criteria (18, 19). Hepatic fibrosis was evaluated by Azan staining. Percentages of fibrous areas were calculated microscopically using an image analysis system (BIOREVO BZ-9000: KEYENCE Japan). Immunohistochemical (IHC) staining was conducted by an immunoperoxidase technique with an Envision kit (DAKO). Primary antibodies used were: rabbit polyclonal PDGFR-α (1:100 dilution), PDGFR-β (1:100 dilution), VEGFR1 (1:100 dilution), desmin (1:100 dilution), β-catenin (1:200 dilution), and mouse monoclonal cyclin D1 (1:400 dilution; all from Cell Signaling Technology); collagen 1 (1:100 dilution), collagen 4 (1:100 dilution), CD31 (1:100 dilution), and CD34 (1:100 dilution; all from Abcam, Cambridge, MA); and Tie-2 (1:80 dilution) and Myc (1:100 dilution; both from Santa Cruz Biotechnology).

Published OnlineFirst May 31, 2012; DOI:10.1158/0008-5472.CAN-12-0028

Quantitative real-time detection PCR

Total RNA was isolated from frozen liver tissue samples using a GenElute Mammalian Total RNA Miniprep Kit (Sigma-Aldrich) according to the manufacturer's protocol. cDNA was synthesized from 100 ng total RNA using a high-capacity cDNA reverse transcription kit (Applied Biosystems) then mixed with the TaqMan Universal Master Mix (Applied Biosystems) and each TaqMan probe. TaqMan probes used were PDGFR-α/β, VEGFR1/2, α-SMA, collagen 1/4, β-catenin, CyclinD1, and Myc (Applied Biosystems). Relative expression levels were calculated after normalization to glyceraldehyde-3-phosphate dehydrogenase (GAPDH).

Western blotting

Western blotting was conducted as described previously (20). Whole-cell lysates from mouse liver were prepared and lysed by CelLytic MT cell lysis reagent (Sigma-Aldrich) containing Complete Mini EDTA-free Protease Inhibitor cocktail tablets (Roche). Cytoplasmic and nuclear protein extracts were prepared using the NE-PER nuclear extraction reagent kit (Pierce Biotechnology). Primary antibodies used were PDGFR-α (1:1,000 dilution), PDGFR-β (1:1,000 dilution), VEGFR2 (1:1,000 dilution), p44/42 MAPK (1:1,000 dilution), total AKT (1:1,000 dilution), p-p44/42 MAPK (1:1,000 dilution), p-AKT (Ser473; 1:1,000 dilution), p-AKT (Thr308; 1:1,000 dilution), β-catenin (1:2,000 dilution), cyclin D1 (1:400 dilution), and lamin A/C (1:1,000 dilution; all Cell Signaling Technology); α-SMA (1:200 dilution; DAKO); 4-HNE (1:200 dilution; NOF); and GAPDH (1:1,000 dilution) and Myc (1:1,000 dilution; both Santa Cruz).

Statistical analysis

Results are expressed as mean ± SD. Significance was tested by 1-way analysis of variance with Bonferroni's method, and differences were considered statistically significant at $P < 0.05$.

Results

Peretinoin prevented the development of hepatic fibrosis in *Pdgf-c Tg*

To evaluate the HCC chemopreventive effects of peretinoin, we used a mouse model of *Pdgf-c Tg* in which PDGF-C is expressed under the control of the albumin promoter (7). Experimental mice were male mice expressing the PDGF-C transgene (*Pdgf-c Tg*); whereas male mice not expressing the transgene were considered WT. After weaning at week 4, *Pdgf-c Tg* or nontransgenic WT mice were fed a basal diet or a diet containing 0.03% or 0.06% peretinoin. At week 20, mice were sacrificed to analyze the progression of hepatic fibrosis. At week 48, mice were sacrificed to analyze the development of hepatic tumors (Fig. 1A). At week 20, Azan staining showed that predominant pericellular fibrosis had developed in *Pdgf-c Tg* mice (Fig. 1B). Densitometric analysis showed a significant dose-dependent reduction in the size of the fibrotic area in mice that received a diet containing peretinoin at both weeks 20 and 48 (Fig. 1C). Peretinoin therefore efficiently repressed the development of hepatic fibrosis in *Pdgf-c Tg* mice.

The expression of fibrosis-related genes in *Pdgf-c Tg* mice was evaluated by IHC staining, quantitative real-time detection PCR (RTD-PCR), and Western blotting. The expression of PDGFR-α and PDGFR-β, essential receptors for intracellular PDGF-C signaling, was upregulated mainly in the intracellular or portal area in *Pdgf-c Tg* mice livers (Fig. 2), but was significantly repressed by peretinoin after weaning at week 4. Similarly, the expression of collagen 1, collagen 4, and desmin was significantly upregulated in *Pdgf-c Tg* mice, but repressed by peretinoin (Fig. 2 and Supplementary Fig. S1A).

RTD-PCR results confirmed that these genes were substantially upregulated in *Pdgf-c Tg* mice and significantly repressed by both 0.03% and 0.06% peretinoin (Fig. 3A). Western blotting showed that the expression of phosphorylated extracellular signal-regulated kinase (p-ERK) 1/2 and cyclin D1, representative markers of the cell proliferation signaling pathway, was upregulated in *Pdgf-c Tg* mice, and repressed by peretinoin (Fig. 3B). Thus, peretinoin could partially but significantly prevent the development of hepatic fibrosis in *Pdgf-c Tg* mice during the study observation period of 48 weeks.

Peretinoin prevented the development of HCC in *Pdgf-c Tg* mice

At week 48, *Pdgf-c Tg* mice developed hepatic tumors with an incidence of 90% (Fig. 4A). Histologic assessment of these tumors verified that 54% (15/28) were adenomas and 46% (13/28) were HCC (Fig. 4A and C and Supplementary Fig. S2; ref. 21). Peretinoin (0.03%) dose-dependently repressed the incidence of hepatic tumors to 53% (19/36) and to 29% (5/17) at 0.06%. Correlating with tumor incidence, maximum tumor size and liver weight were also significantly repressed by peretinoin (Fig. 4B). Thus, peretinoin repressed the development of hepatic tumors in *Pdgf-c Tg* mice.

Serial gene expression profiling in the liver of *Pdgf-c Tg* mice that developed hepatic fibrosis and tumors

To examine which signaling pathways were altered during the progression of hepatic fibrosis and tumor development, we analyzed gene expression profiling in the liver of *Pdgf-c Tg* mice using Affymetrix gene chips. By filtering criteria for $P < 0.001$ and more than 2-fold differences, 538 genes were selected as differentially expressed. One-way hierarchical clustering analysis of differentially expressed genes is shown in Supplementary Fig. S3.

Of the 3 main clusters, 2 were upregulated (clusters A and B) and 1 was downregulated (cluster C). Cluster A consisted of immune-related [chemokine (C-C motif) receptor (CCR)4, CCR2, toll-like receptor (TLR)3 and TLR4], apoptosis-related [caspase (CASP)1 and CASP9], angiogenesis- and/or growth factor–related (PDGF-C, VEGF-C, osteopontin, HGF), oncogene-related [v-ets erythroblastosis virus E26 oncogene homologue (Ets)1, Ets2, CD44, N-myc downstream-regulated (NDRG)1], and fibrosis-related (tubulin) genes. The expression of cluster A genes was further upregulated in tumors at week

Published OnlineFirst May 31, 2012; DOI:10.1158/0008-5472.CAN-12-0028

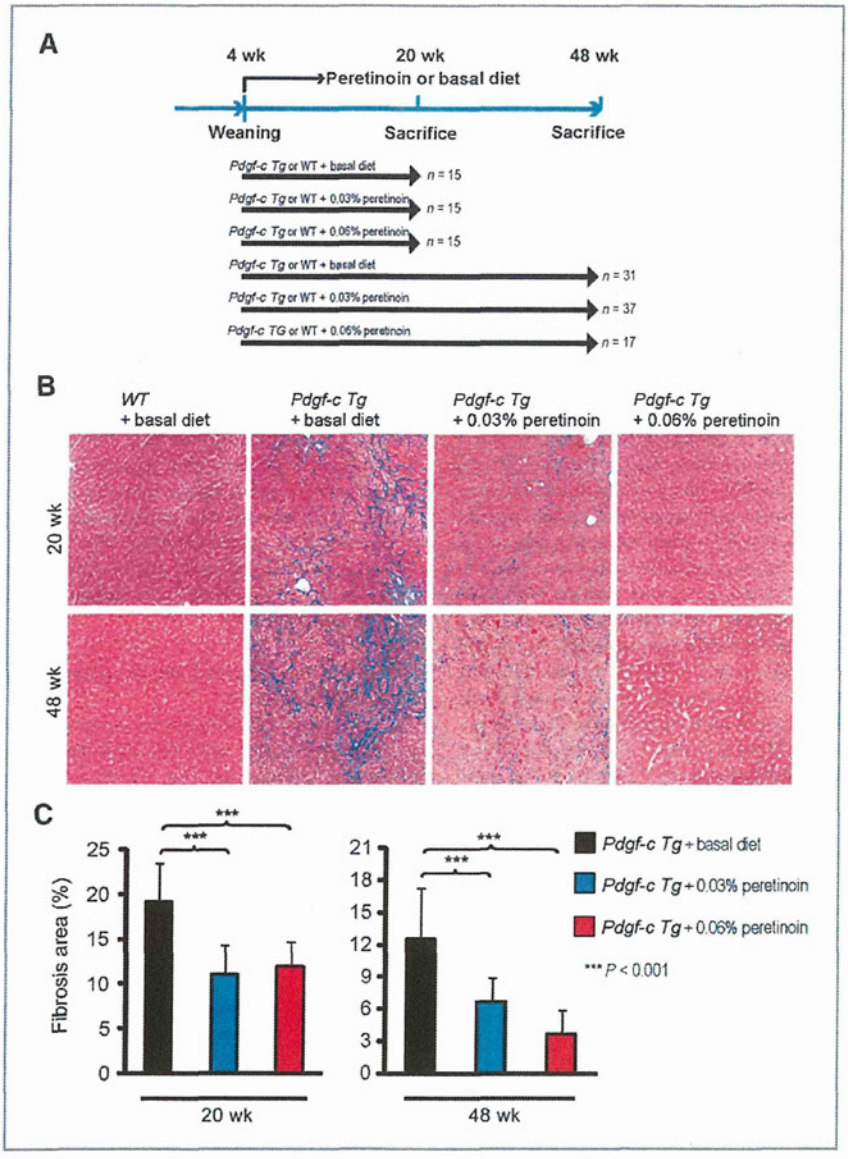

Figure 1. A, feeding schedule of *Pdgf-c Tg* and WT mice. After weaning, male mice were randomly divided into 3 groups: (i) *Pdgf-c Tg* or WT mice receiving basal diet, (ii) *Pdgf-c Tg* or WT mice receiving 0.03% peretinoin-containing diet, and (iii) *Pdgf-c Tg* or WT mice receiving 0.06% peretinoin-containing diet. B, Azan staining of WT or *Pdgf-c Tg* mouse livers fed with different diets at 20 weeks and 48 weeks. C, densitometric analysis of *Pdgf-c Tg* mouse liver fibrotic areas at 20 weeks ($n = 15$) and 48 weeks ($n = 15$).

48. Cluster B consisted mainly of connective tissue- and/or fibrosis-related [vascular cell adhesion molecule (VCAM)1, collagen I, III, IV, V, VI, integrin, decorin, TGF-βRII, PDGFR-α, and PDGFR-β] genes, the expression of which declined slightly at week 48. In contrast, cluster C, containing differentiation and liver function related genes [cytochrome P450, family 2, subfamily c (CYP2C)], were downregulated during the course of hepatic fibrosis and tumor development (Supplementary Fig. S4). Cluster C included xenobiotic- and metabolic process–related genes, which are potential targets of peretinoin. Peretinoin treatment prevented hepatic fibrosis and it preserved liver function. In addition, peretinoin might induce its target genes. Thus, peretinoin reduced the expression of upregulated genes (clusters A and B) and restored the expression of downregulated genes (cluster C) at both weeks 20 and 48 (Supplementary Figs. S3 and S4).

Published OnlineFirst May 31, 2012; DOI:10.1158/0008-5472.CAN-12-0028

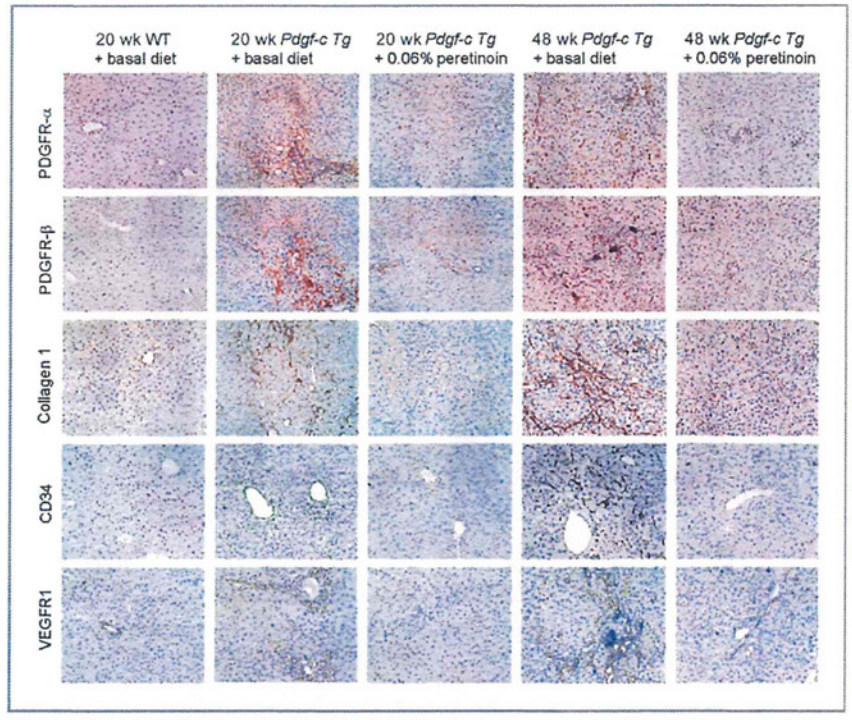

Figure 2. IHC staining of PDGFR-α, PDGFR-β, collagen 1, CD34, and VEGFR1 expression in *Pdgf-c Tg* or WT mouse livers fed a basal diet or 0.06% peretinoin.

To examine the molecular network consisting of differentially expressed genes in *Pdgf-c Tg* mice with or without peretinoin administration, the direct interactions of 513 genes were analyzed by MetaCore (i.e., 413 genes were downregulated and 100 genes were upregulated in *Pdgf-c Tg* mice treated with peretinoin compared with untreated mice; $P < 0.002$). A core gene network consisting of 41 genes was obtained (Supplementary Fig. S5) including interactions between representative growth factors, receptors (PDGFR and TGFβR), and transcriptional factors. Of these genes, the transcriptional factors Sp1 and Ap1 seem to be key regulators in the network (Supplementary Fig. S5).

Peretinoin inhibits PDGFR *in vitro*

Gene expression profiling landscaped the dynamic changes of signaling pathways in *Pdgf-c Tg* mice. To determine the effects of peretinoin *in vitro*, primary HSCs from normal C57BL/6J mice were stimulated by PDGF-C (Fig. 5) to induce the expression of PDGFR-α, PDGFR-β, alpha smooth muscle actin (α-SMA), and collagen 1a2; activated HSCs thus transformed into myofibroblasts (Fig. 5A and B). Peretinoin significantly reduced the expression of these genes and inhibited HSC activation.

We next evaluated the effects of peretinoin on human hepatoma cell lines (Huh-7, HepG2, and HLE), mouse embryonic fibroblast cells (NIH3T3), HUVECs, and Lx-2 (ref. 22; Supplementary Fig. S6A). Experimental conditions were optimized so that more than 90% of cells were variable at 20 μmol/L peretinoin, as determined by an MTS cell proliferation assay (data not shown). Peretinoin dose-dependently inhibited the expression of PDGFR-α and PDGFR-β in Huh-7, HepG2, HLE, NIH3T3, HUVEC, and Lx-2 cells, whereas no obvious expression of PDGFR-α was observed in HepG2 cells and HUVECs (Supplementary Fig. S6A). Peretinoin also inhibited VEGFR2 expression in HUVEC. These results were confirmed by RTD-PCR (data not shown). Correlating with these results, the expression of phosphorylated serine/threonine kinase AKT (p-AKT) and p-ERK1/2, downstream signaling molecules of PDGFR-α, PDGFR-β, and VEGFR2, was also dose-dependently repressed. The expression of collagen 1a2 was significantly repressed by peretinoin in Lx-2, HLE, and Huh-7 cells (Supplementary Fig. S6B). These results suggest that peretinoin may inhibit hepatic fibrosis, angiogenesis, and tumor growth through reduction of the PDGF and VEGF signaling pathway.

We examined the expression of 2 key regulators in peretinoin signaling, Sp1 and Ap1, in Huh-7 cells. Interestingly, the expression of Sp1 was decreased, which correlates with that of PDGFR-α, whereas expression of phosphorylated c-Jun (p-c-Jun) was increased in Huh-7 cells (Supplementary Fig. S6C). Therefore, peretinoin seems to repress the expression of PDGFR, partially through the inhibition of Sp1.

Peretinoin inhibits hepatic angiogenesis in *Pdgf-c Tg* mice

The effect of peretinoin on liver angiogenesis in *Pdgf-c Tg* mice was further analyzed. IHC staining of *Pdgf-c Tg* mouse

Published OnlineFirst May 31, 2012; DOI:10.1158/0008-5472.CAN-12-0028

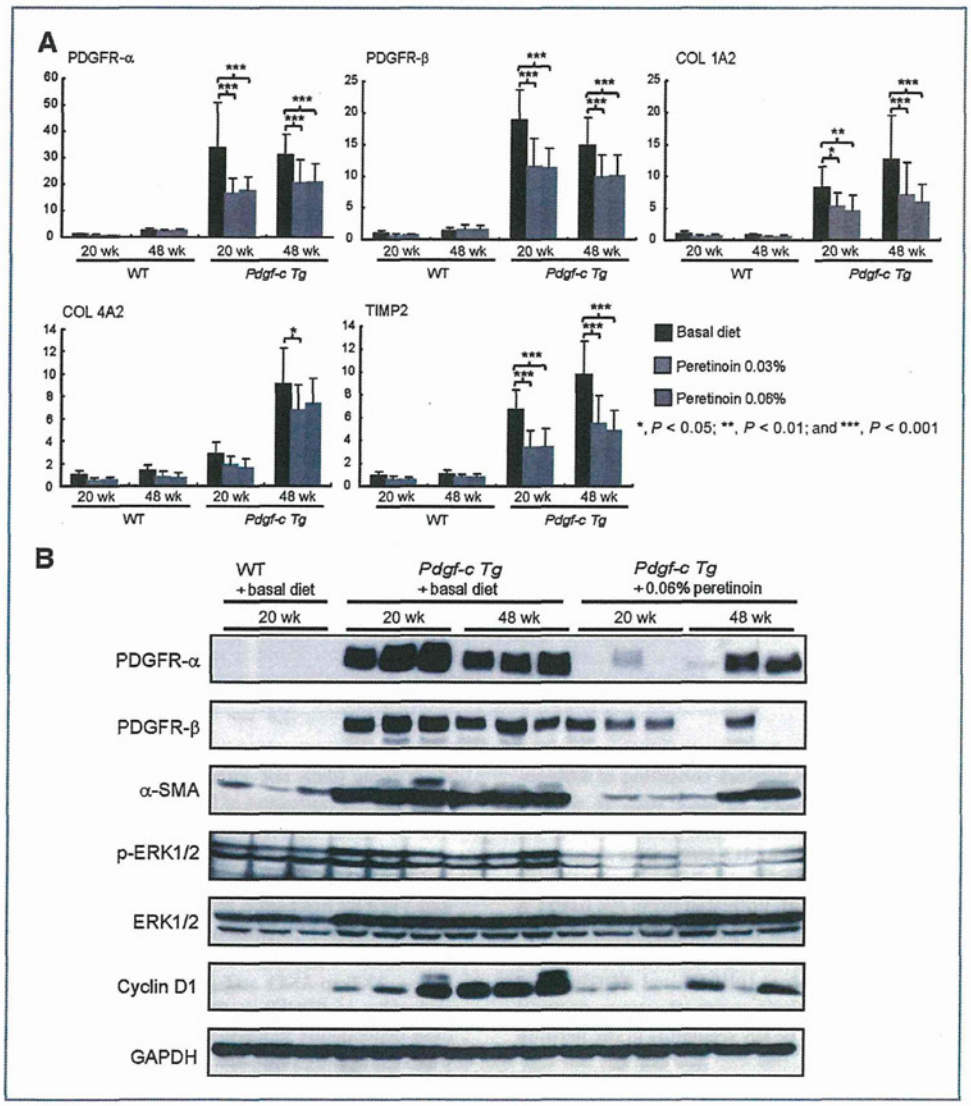

Figure 3. A, RTD-PCR analysis of PDGFR-α, PDGFR-β, collagen (COL) 1a2, collagen 4 a2, and TIMP2 expression in *Pdgf-c Tg* ($n = 5$) or WT mouse livers ($n = 15$). B, Western blotting of PDGFR-α, PDGFR-β, α-SMA, p-ERK, ERK, cyclin D1, and GAPDH expression in PDGF-C Tg or WT mouse livers fed a basal diet or 0.06% peretinoin at 20 or 48 weeks ($n = 3$).

livers at weeks 20 and 48 revealed overexpression of the endothelial markers CD31 and CD34 and the endothelial growth factors VEGFR1 and endothelium-specific receptor tyrosine kinase 2 (Tie2) in the mesenchymal region (Fig. 6 and Supplementary Fig. S1A). This expression was significantly repressed by peretinoin as determined by the densitometric area (Supplemental Fig. S1B). RTD-PCR results revealed significant upregulation of VEGFR1 (Flt-1) in *Pdgf-c Tg* mice compared with WT mice at both weeks 20 and 48, whereas the expression of VEGFR2 (Flk-1) and Tie2 was only upregulated at week 48. The expression of these genes was significantly repressed by peretinoin (Fig. 6A). Western blotting confirmed the upregulation of CD31 and VEGFR1 (Flk-1) at week 48 (Fig. 6B). In addition, p-AKT (Thr 308 and Ser 473) and 4-hydroxy-2-nonenal (4-HNE), an oxidative stress marker, were upregulated in *Pdgf-c Tg* mice and repressed by peretinoin (Fig. 6B).

We also assessed circulating endothelial cells (CEC), a useful biomarker for angiogenesis in the blood, and found that the $CD31^+/CD34^+$ CEC population was significantly upregulated in *Pdgf-c Tg* mice at week 48 but significantly repressed by peretinoin (Fig. 6C and D). Thus, peretinoin

Published OnlineFirst May 31, 2012; DOI:10.1158/0008-5472.CAN-12-0028

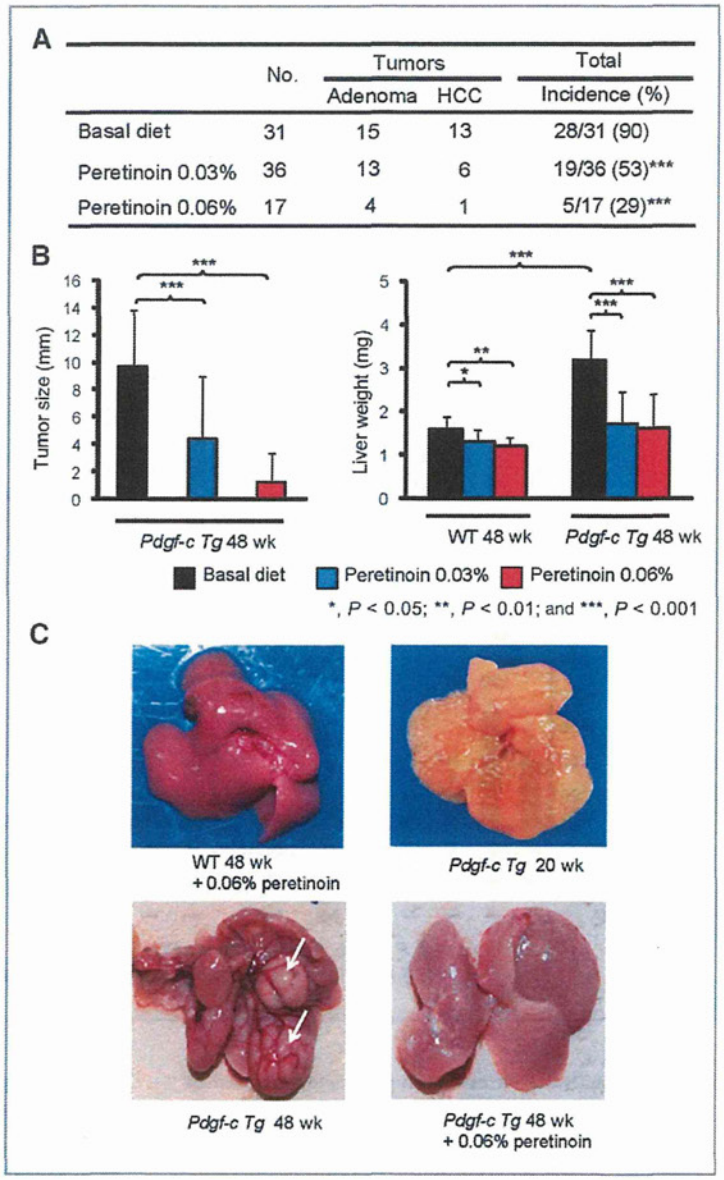

Figure 4. A, incidence of hepatic tumors (adenoma or HCC) in *Pdgf-c Tg* mouse livers fed with different diets. B, tumor sizes and liver weights of *Pdgf-c Tg* and WT mice fed with basal diet ($n = 31$ for *Pdgf-c* Tg, $n = 15$ for WT mice) or 0.03% ($n = 36$ for *Pdgf-c* Tg, $n = 15$ for WT mice) and 0.06% ($n = 17$ for *Pdgf-c* Tg, $n = 15$ for WT mice) peretinoin at 48 weeks. C, macroscopic findings of *Pdgf-c Tg* or WT mouse livers. No obvious change was observed in the liver of WT mice fed with 0.06% peretinoin for 48 weeks (top left). Fibrosis and steatosis were observed in the liver of *Pdgf-c Tg* mice fed a basal diet for 20 weeks (top right). Multiple tumors developed (white arrows) in the liver of *Pdgf-c Tg* mice fed a basal diet for 48 weeks (bottom left). Suppression of tumor development in the liver of *Pdgf-c Tg* mice fed a 0.06% peretinoin diet for 48 weeks (bottom right).

seems to inhibit angiogenesis in the liver of *Pdgf-c Tg* mice, which might prevent the development of hepatic tumors.

Peretinoin inhibits canonical Wnt/β-catenin signaling in *Pdgf-c Tg* mice

The activation of the Wnt/β-catenin signaling pathway is seen in 17% to 40% of patients with primary HCC (23, 24). Moreover, recent reports suggested an interaction between PDGF signaling and Wnt/β-catenin signaling (25–27). We evaluated Wnt/β-catenin signaling in *Pdgf-c Tg* mice and showed by IHC staining that β-catenin was overexpressed in the submembrane at week 48 (Fig. 7A). Peretinoin significantly reduced this expression (Fig. 7A and B), and Western blotting revealed that accumulation of β-catenin in the nuclear fraction of liver tumor tissues was more preferentially repressed by peretinoin than in the cytoplasmic fraction, although expression was repressed in both fractions (Fig. 7C). Wnt ligand (Wnt5a) and frizzled receptor (Fzd1) expression was significantly upregulated in hepatic tumors compared with normal liver (Fig. 7D). These results together suggest that canonical Wnt/β-catenin

Published OnlineFirst May 31, 2012; DOI:10.1158/0008-5472.CAN-12-0028

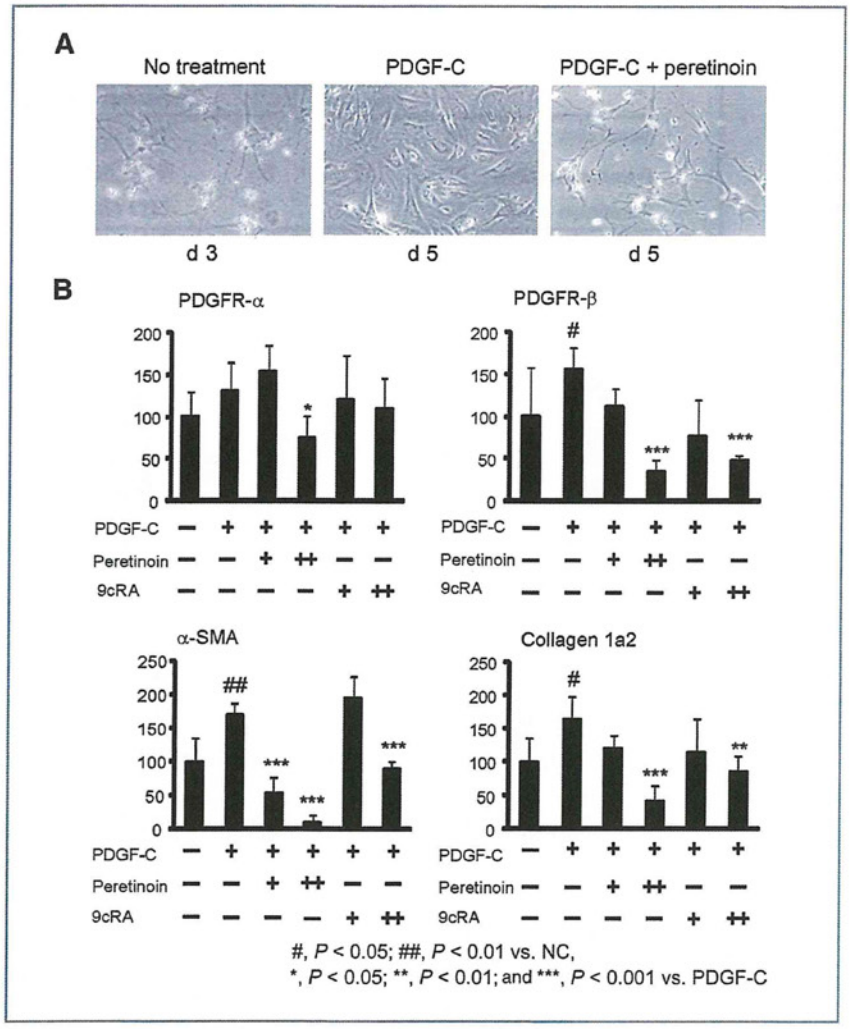

Figure 5. A, microscopic view of freshly isolated primary mouse HSCs after PDGF-C transformation into myofibroblasts (left). Peretinoin inhibited the transformation of HSCs by PDGF-C. B, RTD-PCR analysis of PDGFR-α, PDGFR-β, α-SMA, and collagen 1a2 expression in HSCs treated with or without PDGF-C, peretinoin, and 9cRA ($n = 4$). PDGF-C (+), 80 ng/mL; peretinoin (+), 5 μmol/L; (++), 10 μmol/L; 9cRA (+), 5 μmol/L; (++), 10 μmol/L. NC, no control.

signaling is activated in hepatic tumors and repressed by peretinoin.

Growth factors such as PDGF or HGF potentially activate Wnt/β-catenin signaling (26, 28), which promotes cancer progression and metastasis. We evaluated whether such growth factor signaling could be repressed by peretinoin in hepatic tumors. The expression of c-myc, β-catenin, Tie2, Fit-1, and Flk-1 were significantly upregulated from 1.5- to 4-fold in hepatic tumors compared with normal liver, and this expression was significantly repressed by peretinoin. Similarly, the expression of PDGFR-α, PDGFR-β, collagen 1a2, collagen 4a2, tissue inhibitor of metalloproteinase 2 (TIMP2), and cyclin D1 was substantially upregulated from 5- to 15-fold in hepatic tumors, and significantly repressed by peretinoin (Fig. 7D). Thus, growth factor signaling as well as canonical Wnt/β-catenin signaling in hepatic tumors seems to be repressed by peretinoin. These results explain the inhibitory effect of peretinoin in the development of HCC in *Pdgf-c Tg* mice.

Discussion

HCC often develops in association with liver cirrhosis and its high recurrence rate leads to poor patient prognosis. Indeed, the 10-year recurrence-free survival rate after liver resection for HCC with curative intent was shown to be only 20% (29). Therefore, there is a pressing need to develop effective preventive therapy for HCC recurrence to improve its prognosis.

Peretinoin, a member of the acyclic retinoid family, is expected to be an effective chemopreventive drug for HCC (11, 12, 30) as shown by a previous phase II/III trial in which 600 mg peretinoin per day in the Child-Pugh A subgroup reduced the risk of HCC recurrence or death by 40% [HR = 0.60 (95% CI, 0.40–0.89); ref. 31]. However, further clinical

Published OnlineFirst May 31, 2012; DOI:10.1158/0008-5472.CAN-12-0028

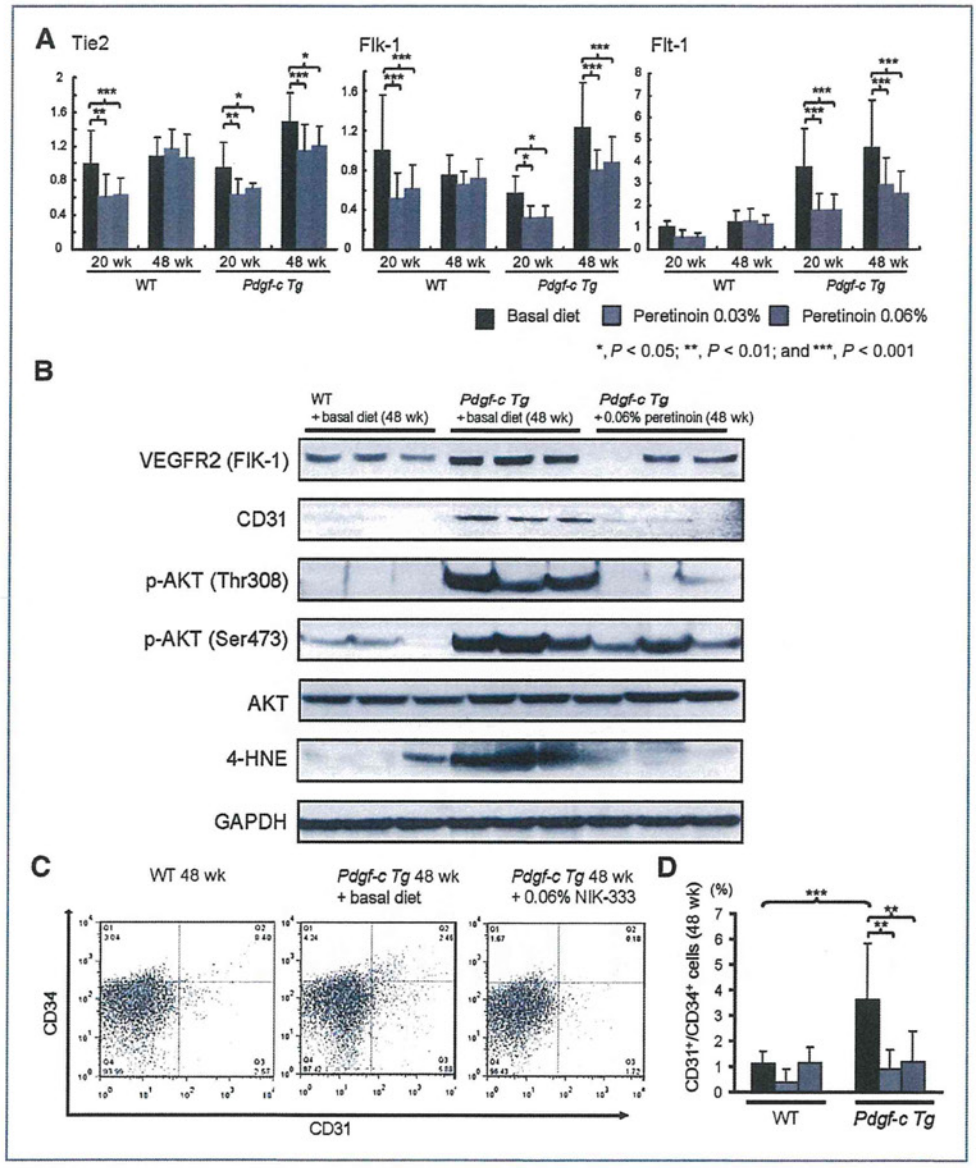

Figure 6. A, RTD-PCR analysis of Tie2, Flk-1, and Flt-1 expression in the liver of *Pdgf-c Tg* and WT mice fed with different diets ($n = 15$). B, Western blotting of Flk-1, CD31, p-AKT (Thr 308, Ser473), AKT, 4-HNE, and GAPDH expression in the liver of *Pdgf-c Tg* or WT mice fed a basal diet or 0.06% peretinoin at 48 weeks ($n = 3$). C, fluorescence-activated cell-sorting analysis of CD31- and CD34-positive CEC in blood of *Pdgf-c Tg* or WT mice fed a basal diet or 0.06% peretinoin at 48 weeks. D, frequency of CD31- and CD34-positive CEC in blood of *Pdgf-c Tg* or WT mice fed a basal diet or 0.06% peretinoin at 48 weeks ($n = 10$).

studies are needed to confirm the clinical efficacy of peretinoin, and a large scale study involving several countries is currently being planned.

During the course of chronic hepatitis, nonparenchymal cells including Kupffer, endothelial and activated stellate cells release a variety of cytokines and growth factors that might accelerate hepatocarcinogenesis. Although peretinoin has been shown to suppress the growth of HCC-derived cells by inducing apoptosis and differentiation (32–35), increasing p21 and reducing cyclin D1 (13), limited data have been published about its effects on hepatic mesenchymal cells such as stellate cells and endothelial cells (14).

In parallel with a phase II/III trial, we conducted a pharmacokinetics study of peretinoin focusing on 12